JOURNAL OF GEOPHYSICAL RESEARCH, VOL. 101, NO. D19, PAGES 23,631–23,650, OCTOBER 30, 1996

Regional atmospheric aerosol composition and sources in the eastern Transvaal, South Africa, and impact of biomass burning

Willy Maenhaut, Imre Salma,[1] and Jan Cafmeyer
Institute for Nuclear Sciences, University of Gent, Gent, Belgium

Harold J. Annegarn
Schonland Research Center for Nuclear Sciences, University of the Witwatersrand, Johannesburg, South Africa

Meinrat O. Andreae
Biogeochemistry Department, Max Planck Institute for Chemistry, Mainz, Germany

Abstract. As part of the Southern Africa Fire-Atmosphere Research Initiative (SAFARI-92), size-fractionated aerosol samples were collected during September-October 1992 at three fixed ground-based sites in the eastern Transvaal, i.e., at two sites within the Kruger National Park (KNP) and at a third site on the Transvaal highveld (about 150 km WSW of the KNP sites), and near a number of prescribed fires in the KNP. The collection devices consisted of stacked filter units, which separate the aerosol into a coarse (2–10 μm equivalent aerodynamic diameter (EAD)) and a fine (<2 μm EAD) size fraction, and of eight-stage cascade impactors, which provide more detailed size fractionation. The samples were analyzed for particulate mass (PM), black carbon (BC), and up to 47 elements. The prescribed fires gave rise to high levels of airborne soil dust, but several species (elements) were particularly enriched in the pyrogenic emissions. This was the case for BC, P, K, Ca, Mn, Zn, Sr, and I in the coarse fraction, and for BC, the halogens (Cl, Br, I), K, Cu, Zn, Rb, Sb, Cs, and Pb (and in the flaming phase also Na and S) in the fine fraction. The aerosol concentrations, compositions, and time trends at the two KNP sites were quite similar, suggesting that regionally representative samples were collected. Receptor modeling calculations, using both absolute principal component analysis and chemical mass balance, indicated that the KNP coarse PM was essentially attributable to mineral dust and sea salt, with average relative apportionments of 75% and 25%, respectively. At the highveld site, mineral dust and sea salt contributed in a 99-to-1 ratio to the coarse PM. In the fine size fraction at all three fixed sites, four components were identified, i.e., mineral dust, sea salt, biomass burning products, and sulfate. The pyrogenic component was the dominant contributor to the atmospheric concentrations of BC, K, Zn, and I, a major source for PM, Cl, Cu, Br, and Cs, but only a minor source for S. About 40% of the fine PM was, on the average, attributed to the pyrogenic particles, and about one third of it to the sulfate component. Relation of the time trends of the various components with three-dimensional air mass back trajectories indicated that elevated levels of pyrogenic products were mostly found in air masses arriving from the north. The levels of the sulfate component tended to be higher at the highveld site than at the two KNP sites, and this component was generally associated with continental air. It was concluded that the major contribution to this fine sulfate came from fossil fuel burning and various industrial activities on the Transvaal highveld.

1. Introduction

Fires in savannas and forested areas, and the burning of fuelwood, charcoal, agricultural waste, and other forms of biomass are increasingly recognized as a globally important source of radiatively and chemically active trace gases and atmospheric particulate material [*Crutzen and Andreae*, 1990; *Levine*, 1991; *Crutzen and Goldammer*, 1993]. Most of the biomass burning takes place in tropical and equatorial regions, where there is a strong seasonality in the extent and frequency of the fire activity. The burning in the tropics, in particular that of savannas, occurs predominantly during the dry season, so that there is a north to south progression of the fire activity over the course of the year, with August through October being the main burning months south of the

[1]Now at Research Institute for Atomic Energy, Budapest, Hungary.

Paper number 95JD02930.
0148-0227/96/95JD-02930$09.00

equator [*Cahoon et al.*, 1992; *Andreae*, 1993a]. The emission of particulate matter during biomass burning occurs mainly in the form of submicrometer, accumulation mode particles (smoke) [*Crutzen and Andreae*, 1990]. These fine particles are efficient scatterers of solar radiation, and, as a consequence, they often have a large impact on local and regional visibility and contribute to the planetary albedo, thus affecting regional and global climate [*Crutzen and Andreae*, 1990; *Andreae*, 1993b]. Moreover, many of the pyrogenic particles can act as cloud condensation nuclei (CCN) [*Rogers et al.*, 1991] and thereby change the radiative properties of clouds. *Penner et al.* [1992] and *Dickinson* [1993] estimated that the combined direct radiative effects of smoke aerosols and the indirect effects through clouds are responsible for a global reflection of solar radiation that is comparable to that from the sulfate aerosol [*Charlson et al.*, 1991, 1992; *Kiehl and Briegleb*, 1993; *Schneider*, 1994].

In order to investigate the role of tropical biomass burning and savanna fires on atmospheric chemistry, climate, and ecology, the Southern Tropical Atlantic Regional Experiment (STARE) was organized as part of the International Global Atmospheric Chemistry (IGAC) Project under the auspices of the International Geosphere/Biosphere Program (IGBP). STARE included as a subprogram the Southern Africa Fire-Atmosphere Research Initiative (SAFARI-92). The field work for SAFARI-92 took place in southern Africa in August, September, and October 1992, during the dry season. The goals of our contribution to SAFARI-92 were to study the amount and composition of aerosol particles produced by biomass burning, to characterize the multielemental composition of aerosols on a regional scale, to identify the major sources of the regional atmospheric aerosol, and to evaluate the relative contribution from these sources, and in particular from biomass burning.

Our activity within SAFARI-92 involved aerosol collections (in two or more size fractions) at a number of ground-based sites (in South Africa, Namibia, and Zimbabwe) and from aircraft, and analysis of the samples by various analytical techniques. Most of the aerosol collections were aimed at obtaining regionally representative samples, but within the Kruger National Park (KNP), South Africa, we also conducted ground-based samplings nearby prescribed savanna fires. In this paper, we present and discuss the results from our ground-based work within the eastern Transvaal and particularly the KNP, South Africa. To aid in the interpretation of our regional aerosol data and to determine quantitatively the contribution from the various source types to the particulate mass and the various aerosol constituents, we relied extensively on receptor models and made use of meteorological information, in particular of air mass back trajectories. The size spectra of the pyrogenic aerosols, their regional distribution, and the concentrations of soluble, ionic species in smoke and ambient aerosols are discussed in detail in companion papers [*Le Canut et al.*, this issue; M. O. Andreae et al., Airborne studies of emissions from savanna fires in southern Africa, 2, Aerosol chemical composition, manuscript in preparation, 1996].

2. Experimental Methods

2.1. Aerosol Samplings

From August 30 until October 12, 1992, size-fractionated atmospheric aerosol samples were continuously collected at three fixed, ground-based sites in the eastern Transvaal, South Africa, i.e., at Skukuza Airport (260 m above sea level (asl)) and Pretoriuskop (600 m asl), which are both located within the Kruger National Park (KNP) in the lowveld (the low altitude savanna area in eastern South Africa), and at Palmer (2000 m asl) on the highveld (the South African high plateau) escarpment. The location of the three sites is shown in Figure 1. The distance from Skukuza to Pretoriuskop is about 40 km and that from Palmer to the two KNP sites about 150 km. Daily (24 hour) aerosol samples were simultaneously taken at all three sites with the "Gent" stacked filter unit (SFU) sampler, and at Skukuza also with an eight-stage PIXE International cascade impactor (PCI). The collections typically started between 0600 and 0730 South African standard time (SAST = UT+2) at Palmer and Skukuza and between 0900 and 1030 SAST at Pretoriuskop.

The "Gent" SFU sampler operates at an airflow rate of 15–16 L/min and works according to the same principles as other SFU variants [*Cahill et al.*, 1977; *Heidam*, 1981; *John et al.*, 1983]. It utilizes two 47-mm-diameter Nuclepore polycarbonate filters, with pore sizes of 8 μm (Apiezon-coated) and of 0.4 μm, which are placed in series. Upstream of the coarse filter is a preimpaction stage, which intercepts the particles larger than 10 μm equivalent aerodynamic diameter (EAD). Consequently, the coarse Nuclepore filter collects the 2–10 μm EAD size fraction, whereas the fine filter collects the particles <2 μm EAD. The PCI used was a 1 L/min, single-orifice, Battelle-type cascade impactor from PIXE International Corporation (Tallahassee, Florida) [*Mitchell and Pilcher*, 1959; *Bauman et al.*, 1981]. More details on this device and the collection surfaces used in it are given elsewhere [*Salma et al.*, 1994]. All SFU samplers and the PCI were set up with their intake facing downward, at about 1.8 m above ground. The air was drawn through the collection devices by means of diaphragm vacuum pumps, and the air volumes were measured with calibrated dry gas meters. All air volumes were converted to cubic meters at standard temperature and pressure (STP; 273.15 K and 1013.2 hPa).

Besides the continuous sampling at the three fixed ("background") sites, we also conducted ground-based collections at a number of prescribed savanna fires in the Pretoriuskop area, i.e., during three burns of small plots and during two large burns (of block 56, on September 18, and of block 55, on September 24). The collections were done with an SFU sampler, and during the block 55 burn also with a PCI. Most of the collections were done during the flaming phase of backing fires, but in each burn we also took one sample during the smoldering phase. The collection time per sample varied from 10 min to 2 hours, and a total of 19 SFU samples were taken over the five burns, and five PCI samples during the block 55 burn.

SAFARI-92 took place after an extended period of drought in South Africa, and there was virtually no precipitation during the 45-day period of our samplings. At the two KNP sampling sites, rainfall occurred only during the 24-hour sampling which started on October 1.

2.2. Analysis

The coarse and fine filters of the SFU samples were analyzed for particulate mass (PM) by gravimetry, for black carbon (BC) by a light reflectance technique [*Andreae*, 1983; *Andreae et al.*, 1984], and for up to 47 elements (from Na to Th) using a combination of instrumental neutron activation

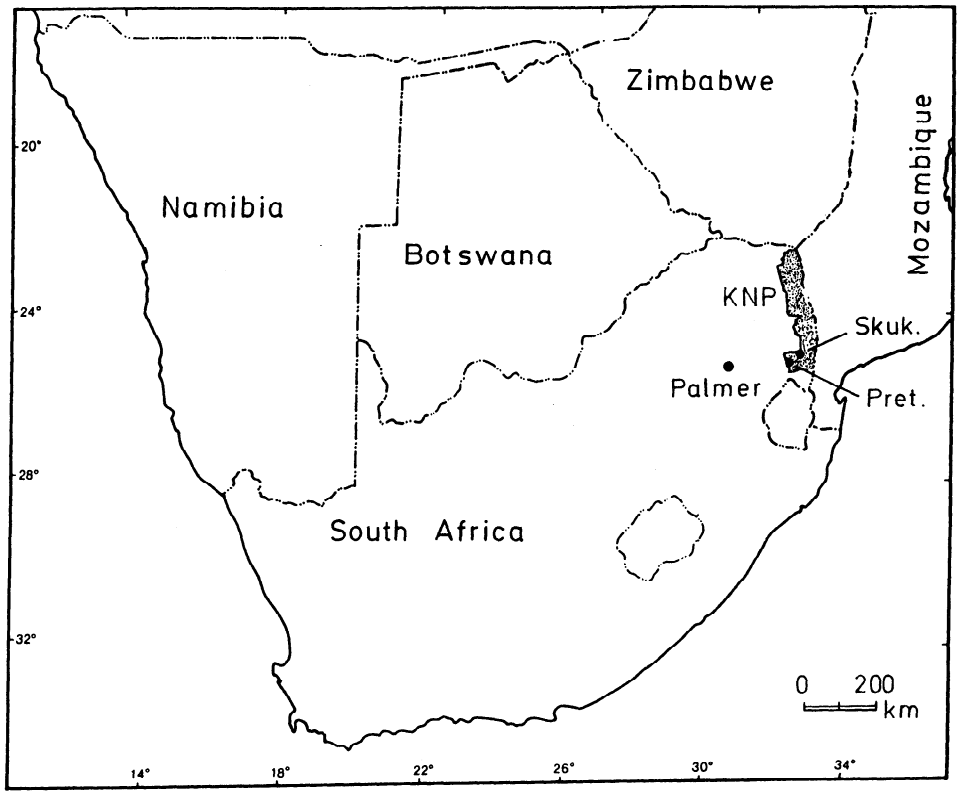

Figure 1. Map with indication of the three fixed SAFARI-92 aerosol sampling sites in the eastern Transvaal, South Africa: Skukuza (260 m asl), Pretoriuskop (600 m asl), and Palmer (2000 m asl).

analysis (INAA) and particle-induced X ray emission analysis (PIXE). The gravimetric analysis was done by weighing each filter before and after sampling with a microbalance (1 μg sensitivity) in a room with stabilized temperature (20°C) and relative humidity (50%). The filters were preequilibrated in this room for at least 24 hours, and during the actual weighing static electricity was eliminated from the filter by means of a ^{210}Po radioactive source. The INAA measurements were done on one half of each filter, and the neutron irradiations, gamma spectrometric counting, and quantification methods were similar to those described by *Maenhaut and Zoller* [1977] and *Schutyser et al.* [1978]. A quarter section of each filter was used for PIXE. The experimental setup and analytical procedures used in these PIXE analyses have been presented before [*Maenhaut et al.*, 1981; *Maenhaut and Raemdonck*, 1984; *Maenhaut and Vandenhaute*, 1986].

The PCI samples were only analyzed by PIXE, with up to 26 elements being looked for. Details on these analyses are given by *Salma et al.* [1994].

2.3. Receptor Modeling

In order to identify the dominant sources (source types) of the particulate mass (PM) and of the various aerosol constituents, and to apportion the PM and the constituents to these sources, we relied extensively on receptor modeling [*Henry et al.*, 1984; *Gordon*, 1988]. We started with a multivariate statistical technique called absolute principal component analysis (APCA), which requires no a priori knowledge on the number and types of particulate sources, and subsequently made use of chemical mass balance (CMB), which enables one to obtain a more accurate source apportionment provided that the major sources are known.

Our APCA method was derived from the procedures of *Thurston and Spengler* [1985] and *Keiding et al.* [1986] and included a VARIMAX rotation of the principal component loading matrix. It is described in detail by *Maenhaut and Cafmeyer* [1987]. For the CMB calculations, we essentially followed the same approach as described by *Lowenthal et al.* [1987], and we made use of an "effective variance" weighing, as proposed by *Watson et al.* [1984].

3. Results and Discussion

3.1. Aerosol Composition and Size Distribution at the Three Fixed, Ground-Based Sites

Table 1 presents the median atmospheric concentrations in the coarse and fine size fractions, as derived from the SFU samples, for each of the three fixed, ground-based sites. Overall, the median levels of the various elements are rather similar at the three sites, thus suggesting that the aerosol compositions are also similar. This similarity in composition is illustrated in Figure 2, which shows the median crustal enrichment factors (EFs), calculated relative to Mason's average crustal rock [*Mason*, 1966] with Al as reference element. It is noteworthy, though, that Na, Mg, Cl, and to a lesser extent, also other sea-salt elements (Ca, Sr, coarse S, and coarse K) exhibit lower EFs at the highveld site (Palmer) than at the two lowveld sites (KNP). As discussed in more

Table 1. Median Atmospheric Concentrations for 49 Variables in the Fine and Coarse Size Fraction of the SFU Samples From Three Fixed, Ground-Based Sites in the Eastern Transvaal during SAFARI-92

Variable	Fine Fraction			Coarse Fraction		
	Skukuza (N=41)*	Pretoriuskop (N=40)	Palmer (N=42)	Skukuza (N=41)	Pretoriuskop (N=40)	Palmer (N=42)
PM	9400	12300	18000	16200	19400	15200
BC	1080	1200	2200	320	390	540
Na	540	430	184	1350	1160	300
Mg	92	75	63	290	280	129
Al	75	138	250	630	950	1060
Si	157	300	440	1210	2000	1900
P†				13.0	19.9	27
S	930	1020	1340	230	210	167
Cl	52	42	22	1670	1300	51
K	220	220	340	182	280	199
Ca	34	35	38	187	260	200
Sc	0.0166	0.021	0.057	0.118	0.153	0.23
Ti	5.7	10.7	15.6	44	70	63
V	0.43	0.50	0.60	1.01	1.40	2.1
Cr	<3	<3	<4	1.82	2.7	5.8
Mn	1.31	2.4	4.0	9.4	16.6	17.2
Fe	51	85	167	370	520	660
Co	0.078	0.090	0.139	0.191	0.32	0.39
Ni	<0.3	<0.4	<0.4	<0.4	0.79	1.25
Cu	0.41	0.68	0.78	0.86	1.75	1.34
Zn	2.1	2.9	5.2	2.3	2.7	2.9
Ga	<0.3	<0.3	0.21	<0.4	<0.3	0.35
Ge†				<0.3	<0.4	<0.4
As	0.125	0.126	0.178	0.112	<0.13	0.088
Se	0.61	0.29	<0.8	<0.3	<0.5	<0.5
Br	8.2	8.6	10.9	3.4	4.1	2.0
Rb	0.71	1.01	1.00	0.94	1.13	1.17
Sr	<0.7	<0.8	<0.8	2.7	4.0	2.1
Y	<0.7	<0.8	<1.0	<0.8	<1.0	<1.1
Zr	<0.9	<1.0	<1.3	1.57	2.4	2.5
Nb	<0.7	<0.9	<1.0	<1.0	<1.0	<1.2
Mo	<0.6	<0.8	<0.6	<0.6	<0.8	<0.5
Ag	<0.3	<0.2	<0.3	<0.2	<0.3	<0.3
Cd	<1.4	<1.4	<1.2	<1.2	<1.3	<0.9
In	<0.008	<0.008	<0.007	<0.015	<0.014	<0.009
Sn	<13	<14	<16	<20	<30	<20
Sb	0.048	0.128	0.158	0.066	0.061	0.116
I	2.1	2.1	2.7	0.67	0.63	0.55
Cs	0.054	<0.005	0.075	0.056	0.073	0.076
Ba	<7	<8	<9	12.3	16.3	10.5
La	0.082	0.114	0.152	0.46	0.63	0.61
Ce	<1.0	<0.9	<1.3	1.12	1.91	<2
Sm	0.0102	0.0150	0.025	0.075	0.103	0.102
Eu	<0.03	<0.02	<0.03	0.021	0.037	0.024
Lu	<0.02	<0.02	<0.02	<0.018	<0.02	0.0133
W	<0.11	<0.05	<0.09	<0.04	<0.06	0.082
Au	<0.0017	<0.002	<0.0017	0.00168	<0.0018	<0.0010
Pb	3.4	4.5	6.0	1.24	1.61	2.1
Th	<0.08	0.050	0.102	0.103	0.175	0.22

Values are in nanograms per cubic meter STP.
*N indicates the number of SFU samples on which the medians are based.
†The elements P and Ge were not determined in the fine filters of the SFU samples.

detail below, Palmer was much less impacted by sea-salt aerosol than KNP.

Most elements in the coarse size fraction (Figure 2a) have crustal EFs that are very close to one, thus suggesting that they are mainly attributable to soil dust dispersal. Interestingly, the list of nonenriched elements includes Mg, Si, P, K, Ca, Mn, Rb, and Sr, which are often enriched owing to natural biogenic emissions and/or to biomass burning in continental equatorial/tropical regions [*Maenhaut and Akilimali*, 1987; *Artaxo et al.*, 1988, 1993]. Moreover, Si, Ca, and Mn are also not enriched in the fine size fraction (Figure 2b), whereas the levels of P and Sr were below the detection limit in that size fraction. The metals and metalloids Cu, Zn, As, Se, Sb, and Pb generally exhibit high EF values in industrialized countries (where they are attributed to a variety of anthropogenic sources), but they are also highly enriched in the remote marine atmosphere and even at the geographic south pole [e.g., *Maenhaut et al.*, 1979; *Arimoto et al.*,

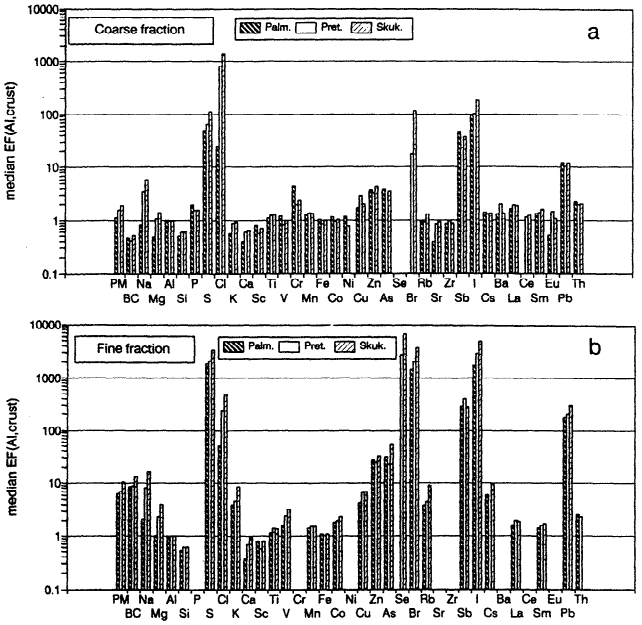

Figure 2. Median crustal enrichment factors (EFs), calculated relative to Mason's average crustal rock [*Mason*, 1966] with Al as reference element, for 37 species at the three fixed sites (a) for the coarse size fraction (2–10 μm EAD) and (b) for the fine size fraction (<2 μm EAD). The data displayed for black carbon (BC) are concentration ratios to Al instead of EFs.

1987]. Figure 2 shows that the EFs of these elements are only moderate in the coarse fraction (except for Sb), but significantly larger in the fine fraction.

Because of the similarities in both the fine and coarse aerosol compositions at the three fixed sites, the fine-to-coarse elemental concentration ratios were also similar. This is demonstrated in Figure 3, which displays the average fine/coarse ratios. This figure also shows that the typical mineral dust elements Al, Si, Ca, Ti, Mn, and Fe have a fine/coarse ratio of about 0.2 at the three sites; for the sea-salt elements Na, Mg, and Sr, and for V and Cu, the ratio is of the order of 0.3-0.5; and PM, BC, S, K, Zn, As, Se, Br, Rb, Sb, I, and Pb exhibit ratios of 1 or higher (about 4 for

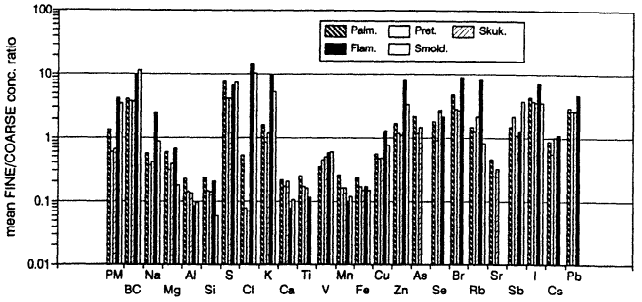

Figure 3. Average fine/coarse concentration ratios for 25 particulate species at the three fixed SAFARI-92 sampling sites and in aerosols collected during the flaming and smoldering phase near prescribed savanna fires in the Pretoriuskop area.

BC, S, Br, I, and Pb). For Cl, a very low fine/coarse ratio (of about 0.07) is observed at the two KNP sites, and, in addition, it is much lower than that for Na. From a comparison of the PCI and SFU data for Skukuza, it appeared that about 10 times more Cl was observed in the fine fraction with the PCI than with the SFU, presumably because of Cl losses from the fine SFU filters during the sampling or between sampling and analysis [*Salma et al.*, 1994]. In the Skukuza PCI data set an average fine/coarse ratio of 0.22 was noted for Cl. Another indication for the Cl loss from the fine SFU filters was provided by a comparison with the data for water-soluble ions in background samples collected during regional flights. The Cl^-/SO_4^{2-}-S ratio in the fine size fraction of the latter samples was about 5 (M. O. Andreae et al., Airborne studies of emissions from savanna fires in southern Africa, 2, Aerosol chemical composition, manuscript in preparation, 1996), whereas the Cl/S ratio in the fine SFU filters was of the order of only 0.05.

The Skukuza PCI data set was used to derive average mass size distributions and average mass median aerodynamic diameters (MMADs) for up to 24 elements [*Salma et al.*, 1994]. The MMADs were obtained for every individual sample by plotting (on a lognormal probability graph) the percentage cumulative mass of an element versus the cut diameter (d_{50} value) of the stage just above the stage up to which the data were summed, and by then linearly inter-

Table 2. Average Elemental Mass Median Aerodynamic Diameters and Associated Standard Deviations, as Derived from the PIXE International Cascade Impactor Samples Collected at Skukuza and Near the Prescribed Savanna Fires

Element	Skukuza	Fires	
	(N=41)*	Flaming (N=4)	Smoldering (N=1)
Na	3.5 ± 0.7	1.20 ± 0.60	3.3
Mg	3.6 ± 0.4	6.0 ± 0.7	4.5
Al	5.7 ± 0.8	9.4 ± 1.6	6.6
Si	6.1 ± 0.8	11.6 ± 0.5	6.7
P	6.2 ± 1.2	6.4 ± 0.4	6.5
S	0.78 ± 0.33	0.37 ± 0.10	1.07
Cl	4.0 ± 0.6	0.34 ± 0.07	3.6
K	3.0 ± 1.2	0.32 ± 0.12	1.04
Ca	5.2 ± 0.7	7.3 ± 0.7	6.2
Ti	6.4 ± 0.9	11.0 ± 1.8	6.1
V	5.4 ± 1.4		
Cr	5.8 ± 0.8		
Mn	6.0 ± 0.9	7.2 ± 1.3	5.5
Fe	6.2 ± 0.8	10.1 ± 2.6	6.3
Ni	5.6 ± 0.8		
Cu	5.3 ± 1.3		
Zn	3.6 ± 1.6	0.30 ± 0.08	2.8
Ga	5.5 ± 0.8		
Se	1.48 ± 0.46		
Br	1.13 ± 0.68	0.23 ± 0.02	
Rb	4.8 ± 1.6		
Sr	4.8 ± 0.8	7.2 ± 1.0	5.5
Zr	6.2 ± 1.4		
Pb	0.81 ± 0.38	0.30 ± 0.10	

Values are in micrometers equivalent aerodynamic diameter (EAD).

*N indicates the number of cascade impactor samples on which the data are based.

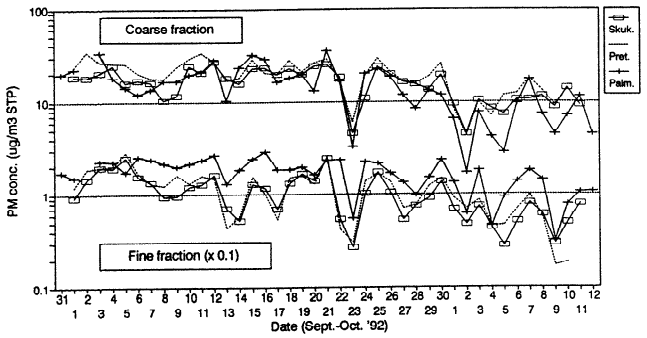

Figure 4. Atmospheric concentrations (in micrograms per cubic meter STP) as a function of sampling date (time trends) for the particulate mass in the coarse and fine size fraction at the three fixed SAFARI-92 sites. The dates on the abscissa indicate the starting day for each sample.

polating between the two data points that are closest to the 50% cumulative mass and extracting the particle diameter that corresponds to that 50% [*Marple et al.*, 1993]. The individual sample MMADs were then used to calculate the average MMAD and associated standard deviation for each element, as listed in Table 2. On the basis of the average size distributions [*Salma et al.*, 1994, Figure 1] and the average MMADs, the 24 elements could be classified in three groups. The first group comprised Na, Mg, Al, Si, P, Cl, Ca, Ti, V, Cr, Mn, Fe, Ni, Cu, Sr, and Zr. All these elements had essentially a unimodal size distribution, most of their mass was present in supermicrometer particles (consistent with the SFU fine/coarse ratios of Figure 3), and their MMADs are of the order of 4 to 6 μm EAD. The elements in the second group (i.e., K, Zn, and Rb) also have a large MMAD (of 3–5 μm EAD), but, in contrast to those in the first group, they clearly had a bimodal size distribution. Also the third group of elements (with S, Br, and Pb) exhibit a bimodal size distribution, but most of their mass is in the fine size fraction (again consistent with the SFU data of Figure 3), and, as a consequence, their MMADs are below (or around) 1 μm EAD.

The atmospheric concentrations in the fine and in the coarse size fractions of the three fixed sites were not only similar on an average basis, but for many particulate species (elements) also on a sample-to-sample basis. This is illustrated in Figure 4, which shows the time trends for coarse and fine PM at the three sites. Overall, the similarity in atmospheric levels and the coherence between the time trends were particularly good in the fine size fraction and between the Skukuza and Pretoriuskop sites. A detailed discussion of this coherence and of its relation with meteorology will be given below.

3.2. Composition and Size Distributions for Particulate Emissions from the Prescribed Savanna Fires

From the data of the SFU collections near the prescribed savanna fires in the Pretoriuskop area, separate median compositions were calculated for the flaming and smoldering fire samples, and for the fine and coarse size fractions. The resulting compositions are given in Table 3. The average fine/coarse ratios for the various particulate species (elements) in the separate flaming and smoldering fire samples are shown in Figure 3, where they are compared with the fine/coarse ratios at the three fixed sites. The compositions of the pyrogenic particles were also examined in terms of crustal EFs and, more specifically, relative to the EFs for the Skukuza site. Skukuza was selected as a "reference" site as it was the only one of our three fixed ("background") sites where both PCI and SFU samples were collected. Consequently, Skukuza could also serve as a "reference" site in comparisons with the PCI samples from near the prescribed fires. The relative EF values are presented in Figure 5.

The data from the PCI collections near the prescribed fires were used to calculate average elemental mass size distributions and MMADs in the same way as for the PCI samples from Skukuza. The average size distributions for the collections during the flaming phase are shown in Figure 6, and the average MMADs for the flaming and smoldering fire samples are given in Table 2. A general feature of the size distributions for the flaming phase PCI samples, when compared to the Skukuza PCI data, is that the maximum in the coarse mode (both for elements with a unimodal and for those with a bimodal size distribution) is shifted toward larger particle sizes, whereas the maximum in the fine mode (for bimodal size distributions) is shifted toward the finer particle sizes. As a result, for the coarse particle elements significantly higher MMADs are seen for the flaming phase samples than for the Skukuza "background" site (see Table 2), whereas S, Cl, K, Zn, Br, and Pb, which all have a very pronounced submicrometer mode in the flaming fire samples (see Figure 6), exhibit a much decreased MMAD. During the smoldering phase, the MMADs of the various elements seem to become similar to the "background" values, but this result should be considered with great caution as only one PCI sample was collected during smoldering fire.

Overall, the results from the flaming phase PCI collections are quite consistent with those from the flaming fire SFU samples. As can be seen in Figure 3, the elements S, Cl, K, Zn, Br, and Pb, which all had a very low MMAD in the flaming fire PCI samples, have a larger (and for Cl, K, and Zn much larger) fine/coarse ratio in the flaming fire SFU samples than at the fixed sites. Furthermore, Na and Rb, for which a distinct fine mode is seen in Figure 6, also have much increased fine/coarse ratios in the flaming fire SFU samples. Finally, an increased fine/coarse ratio during the flaming phase is also found for some particulate species and elements that were not measured in the PCI samples (i.e., for PM, BC, and I). On the basis of the combined PCI and SFU size distribution information it can therefore be concluded that the flaming phase of savanna fires is a prominent source of the following species (elements) in the fine particle fraction: PM, BC, Na, S, Cl, K, Zn, Br, Rb, I, and Pb. For this last element the pyrogenic emission may in fact be a remobilization of material that was present on the savanna (grasses and leaves) as a result of dry deposition from the atmosphere.

The typical mineral dust elements (i.e., Al, Si, Ti, Fe) all have significantly larger MMADs for the flaming phase PCI samples than for the Skukuza "background" (see Table 2). For Al and Ti, the increase in MMAD also gave rise to a decreased fine/coarse ratio (see Figure 3). Moreover, the atmospheric concentrations (in ng/m^3) for the mineral dust elements were all much larger in the flaming fire samples

Table 3. Median Compositions of the Fine and Coarse Aerosol Particles, Collected with SFU Samplers During the Prescribed Fires in the Pretoriuskop Area

Variable	Fine Fraction		Coarse Fraction	
	Flaming (N=14)*	Smoldering (N=5)	Flaming (N=14)	Smoldering (N=5)
BC	310	106	137	44
Na	3.7	1.36	6.2	6.9
Mg	<0.6	<1.0	4.1	10.7
Al	0.175	0.56	14.4	17.6
Si	<1.5	<1.5	47	45
P†			3.1	4.6
S	6.4	3.5	4.6	2.7
Cl	97	23	37	9.2
K	62	17.8	30	15.0
Ca	0.29	0.36	21	27
Sc	<0.0005	<0.0009	0.0021	0.0027
Ti	<0.05	<0.07	0.84	1.25
V	<0.007	<0.005	0.021	0.026
Cr	0.92	1.64	0.152	0.37
Mn	0.0155	0.024	0.80	0.76
Fe	0.195	0.31	5.9	8.5
Co	<0.005	<0.008	<0.015	<0.011
Ni	<0.02	<0.03	<0.07	<0.09
Cu	0.028	<0.03	<0.08	<0.09
Zn	0.45	0.102	0.22	<0.15
Ga	<0.009	<0.005	<0.017	<0.03
As	<0.004	<0.004	<0.006	<0.008
Se	<0.06	<0.09	<0.09	<0.11
Br	0.79	0.193	<0.3	<0.2
Rb	0.043	0.022	0.020	0.075
Sr	<0.03	<0.04	0.33	0.57
Y	<0.04	<0.05	<0.13	<0.15
Zr	<0.04	<0.06	<0.2	<0.2
Nb	<0.05	<0.08	<0.17	<0.2
Mo	<0.04	<0.04	<0.09	<0.09
Ag	<0.019	<0.03	<0.05	<0.07
Cd	<0.08	<0.07	<0.14	<0.14
In	<0.0007	<0.0005	<0.0010	<0.0011
Sn	<0.9	<0.9	<2	<2
Sb	0.00147	0.0040	<0.003	<0.004
I	0.098	0.052	0.055	0.061
Cs	0.00192	0.0060	<0.015	<0.019
Ba	<0.6	<0.5	<1.3	<1.9
La	<0.003	<0.002	0.021	0.030
Ce	<0.14	<0.2	<0.07	<0.14
Sm	<0.0003	<0.0003	0.0022	0.0027
Eu	<0.002	<0.004	<0.006	<0.005
Lu	<0.0013	<0.0018	<0.003	<0.004
W	<0.003	0.0038	<0.005	0.0082
Au	<0.00010	0.00027	0.00019	0.00022
Pb	0.064	0.025	<0.11	<0.11
Th	<0.010	<0.017	<0.008	<0.010

The mass concentrations for the 47 species measured are expressed in milligrams per gram particulate mass.

*N indicates the number of SFU samples on which the medians are based.

†The element P was not determined in the fine filters of the SFU samples.

than at the fixed sites. These various observations indicate that savanna fires are efficient mobilizers of soil dust into the atmosphere, as was recently also found by *Gaudichet et al.* [1995].

Besides the fine/coarse ratios and size distributions the crustal EF values also provide clues to the importance of savanna fires as a source for the various elements. Indeed, when an element has a significantly larger EF value in the pyrogenic aerosol than at the fixed "background" sites, then the burning itself should be a prominent source for that element. By applying this approach to the relative EF values of Figure 5, it is concluded that savanna fires are a major source for the following species in the coarse fraction: PM, BC, P, K, Ca, Mn, Zn, Sr, and I, and this is the case in both the flaming and smoldering phases. Similarly, in the fine fraction, the fires are a major source for PM, BC, Cl, K, Cu, Zn, Br, Rb, Sb, I, Cs, and Pb.

The median compositions for the pyrogenic aerosols from the flaming and smoldering phases, as given in Table 3, were derived from the raw SFU data for the fire samples, and no

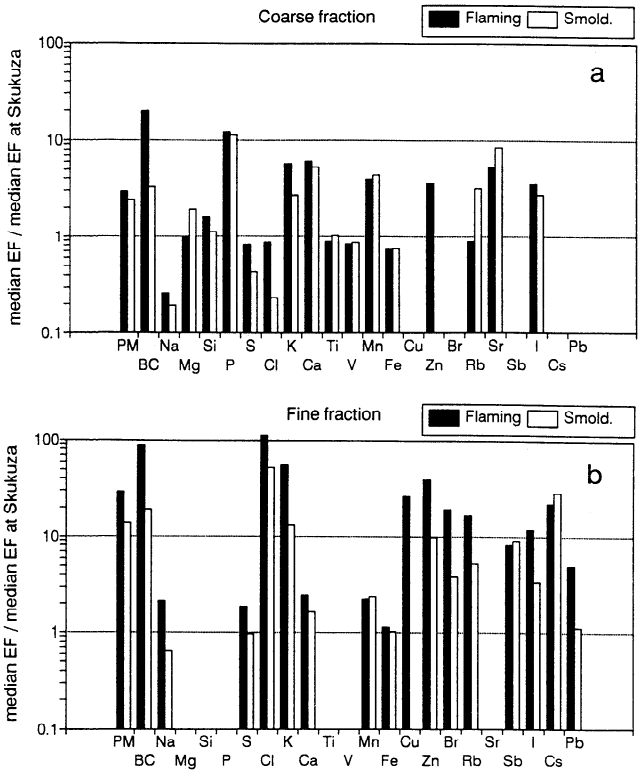

Figure 5. Ratios of median crustal EF values in the pyrogenic particles to the median EFs at the Skukuza site.

correction was applied for the contribution from soil dust that is mobilized by the fires. By assuming that the Al in the fire samples is purely attributable to mineral dust and utilizing ratios of the various elements to Al in average crustal rock or soil, "pure" pyrogenic aerosol profiles may be obtained, as was done by *Gaudichet et al.* [1995] for their data set from prescribed savanna fires in Lamto, Ivory Coast. By applying a similar correction to the data of Table 3, the profiles for the fine fraction would remain fairly unchanged; Al and Fe would disappear, and the concentrations of Mg and Ca would be lowered by a factor of 2 to 3. For the coarse fraction, on the other hand, the correction would give rise to quite drastic alterations: the elements Al, Si, Ti, V, Fe, and Rb would all be eliminated from the two profiles, and the concentrations of Na and Mg would be reduced by a factor of about 4 in the coarse flaming fire profile.

A comparison of the uncorrected profiles for the flaming and smoldering phase aerosols of Table 3 indicates that they are fairly similar for the coarse size fraction, but not for the fine fraction, where most elements have higher concentrations (typically by a factor of about 3) in the flaming phase profile than in the smoldering phase profile. Another interesting comparison is that between the fine and coarse profiles of Table 3. For the flaming phase aerosol, consistently higher concentrations are observed in the fine profile than in the coarse profile for virtually all species that are predominantly associated with the fine size fraction (i.e., BC, S, K, Zn, Br, Rb, I, and Pb).

Until now, only a few multielemental particle emission profiles have been presented in the literature for savanna fires or for other tropical biomass burning. Furthermore, the published data are usually for the total particulate emission (no fine/coarse distinction), include often only results for a few elements (species), and/or are reported in terms of concentration ratios to a typical burning product (e.g., total carbon, K). As a consequence, only a very limited comparison can be made of our uncorrected (or corrected) profiles with literature results. From their measurements at prescribed humid savanna fires in Lamto, *Gaudichet et al.* [1995] derived a flaming phase profile for the total aerosol which included the following elements (with concentrations in milligrams per gram PM): P (1.3), S (2.1), Cl (23), K (31), Cu (0.03), and Zn (0.2). Furthermore, these authors reported that all elements (except P) were for 80% or more associated with the fine size fraction. No information was given, however, on what percentage of the total PM was in the fine fraction, but presumably that was of the same order (in our flaming phase samples we found a fine/coarse ratio of about 4; see Figure 3). Therefore the profile of *Gaudichet et al.* [1995] may be compared with our fine aerosol profile of Table 3. It appears that S, Cl, K, and Zn are all higher by a factor of 2-4 in our profile than in that of *Gaudichet et al.* [1995], whereas the Cu concentration is about the same.

Of the various elements and species that were determined by us, two (i.e., K and BC (or alternatively elemental carbon (EC) or soot carbon)) are often included in other data sets on pyrogenic emissions. *Cachier et al.* [1991] and *Lacaux et al.* [1993] observed in their Dynamique et Chimie de l'Atmosphère en Forêt Equatoriale (DECAFE) studies that the ratio of black carbon to total carbon in the fine fraction of savanna fire aerosol is typically of the order of 0.10-0.15 during the flaming phase, but they occasionally found higher ratios also (of about 0.25), which were tentatively ascribed to be the result of large-scale (higher temperature) fires. For the ratio

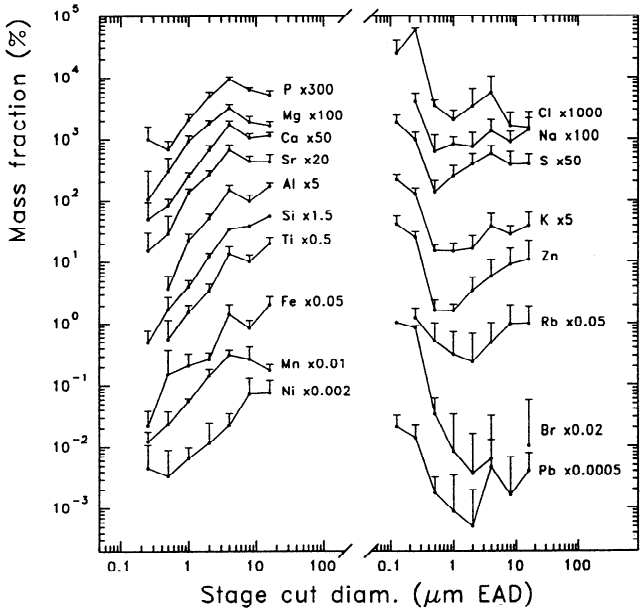

Figure 6. Average mass size distributions for 18 elements in the particles emitted during the flaming phase of prescribed fires. The data are mean mass fractions and standard deviations, based on four cascade impactor samples, collected during the burn of block 55 (on September 24). For the filter stage, the cut diameter (d_{50} value) was set at 0.125 μm EAD.

Table 4. VARIMAX Rotated Loadings for 26 Aerosol Variables and up to Three Meteorological Variables on the Two Retained Components in the Coarse Size Fraction Data Sets of the Three Fixed Sites

	Component 1 (Mineral Dust)			Component 2 (Sea Salt)		
Variable	Skukuza	Pret.*	Palmer	Skukuza	Pret.	Palmer
PM	0.77	0.88	0.89	0.62	0.44	0.42
Na				0.97	0.97	0.95
Mg		0.21	0.75	0.97	0.92	0.58
Al	0.98	0.98	0.91			0.40
Si	0.99	0.99	0.92			0.37
P	0.85	0.93	0.90			0.30
S			0.51	0.91	0.87	0.49
Cl			0.27	0.89	0.86	0.85
K	0.90	0.96	0.89	0.35		0.41
Ca	0.87	0.96	0.90	0.43		0.39
Sc	0.97	0.93	0.91			0.39
Ti	0.98	0.99	0.92			0.38
V	0.97	0.94	0.90			0.39
Mn	0.99	0.96	0.90			0.37
Fe	0.99	0.98	0.91			0.40
Co	0.98	0.98	0.90			0.39
Ni	0.94	0.73	0.87			0.40
Zn	0.92	0.90	0.81			
Rb	0.79	0.70	0.72			
Sr	0.70	0.91	0.81	0.58		0.43
Zr	0.76	0.84	0.80			0.41
I	0.51	0.53	0.72	0.62	0.60	0.45
Cs	0.89	0.85	0.87			0.23
La	0.98	0.98	0.92			0.35
Sm	0.99	0.99	0.93			0.33
Th	0.92	0.98	0.91			0.33
T†	0.55	0.57	0.65			
WS						
P	-0.57					

Loadings which were less than 3 times their associated standard deviation, as calculated according to *Heidam* [1982], loadings with an absolute value of less than 0.2, and negative loadings (for the aerosol variables) are not listed in the table.

*Pret. denotes Pretoriuskop.

†T, WS, and P indicate 24-hour average local temperature, wind speed and pressure, respectively; in the PCAs with the meteorological variables included, all three variables were entered for Skukuza, but for Pretoriuskop and Palmer only T.

of K to total carbon, *Lacaux et al.* [1993] reported a value of about 0.1. Considering that total carbon represents probably about 70% of the fine pyrogenic aerosol [*Crutzen and Andreae*, 1990; *Lacaux et al.*, 1993], the K data of *Lacaux et al.* [1993] is fully consistent with the K concentration in our fine flaming phase profile. For BC, on the other hand, our result appears to be about 2 to 4 times higher than the DECAFE data. This difference may to a large extent be due to differences in the BC measuring techniques. In the DECAFE work BC is determined by a thermal evolution method, whereas our BC data were obtained from a light reflectance measurement. Most likely, the two methods measure different "black carbon" species.

3.3. APCA Receptor Modeling on the Data Sets From the Three Fixed, Ground-Based Sites

The fine and coarse fraction multielement data sets from the SFU collections of each of the three fixed sites were subjected to APCA. Furthermore, principal component analyses (PCA) were performed on coarse fraction data sets in which some meteorological parameters were also included (i.e., 24-hour average local temperature, wind speed, and pressure for Skukuza; and 24-hour average local temperature for Pretoriuskop and Palmer). Of the up to 49 particulate species measured, 26 were retained in the APCA (and PCA) calculations for the coarse fraction. The basic criterion to retain an element for APCA was that it had to be present above the detection limit in at least 80% of the samples. A few elements, for which this criterion was fulfilled and which occurred at minor or trace levels in the particulate material, were excluded because they gave rise to unique components (this was often due to large (outlier) concentrations in a few samples). This was done for Cr, Cu, Sb, and Pb in the coarse fraction (for Cu and Sb because of outliers). The PCA on each of the three coarse fraction data sets indicated that only two components were present. The VARIMAX rotated loadings for the various variables on these components are given in Table 4. The loadings for the aerosol variables are from the PCA with the meteorological variables excluded, but they remained essentially unchanged when the latter were included. The typical mineral dust elements (Al, Si, Sc, Ti, Fe,

Table 5. VARIMAX Rotated Loadings for up to 26 Aerosol Variables on the First Three Components in the Fine Size Fraction Data Sets of the Three Fixed Sites

	Component 1 (Mineral Dust)			Component 2 (Biomass Burning)			Component 3 Sea Salt		Component 3 Sulfate at
Variable	Skukuza	Pret.	Palmer	Skukuza	Pret.	Palmer	Skukuza	Pret.	Palmer
PM	0.52	0.52	0.60	0.79	0.74	0.72	0.22	0.21	0.23
BC	0.36	0.44	0.46	0.91	0.86	0.86			
Na			0.31			0.74	0.97	0.89	
Mg	0.25	0.36	0.73	0.22			0.90	0.86	
Al	0.95	0.90	0.92	0.23	0.34	0.32			
Si	0.94	0.89	0.95	0.25	0.37	0.26			
S	0.64	0.45	0.49	0.33	0.28		0.38	0.52	0.68
Cl						0.93	0.47		
K	0.31	0.41	0.41	0.91	0.87	0.89			
Ca	0.68	0.81	0.92	0.28	0.35	0.30	0.63	0.40	
Sc	0.95	0.85	0.93		0.23	0.25		0.30	
Ti	0.93	0.87	0.93	0.24	0.39	0.31			
V	0.52	0.38	0.87			0.28	0.63	0.71	0.32
Mn	0.95	0.86	0.88	0.23	0.27				0.33
Fe	0.96	0.88	0.92		0.30	0.32		0.23	
Co	0.82	0.90	0.72		0.27				
Zn	0.64	0.60	0.70	0.59	0.55	0.37		0.29	0.56
Se				0.44	0.75		0.57	0.32	0.71
Br	0.42	0.42	0.24	0.71	0.70	0.89	0.39		
Rb		0.32		0.73	0.77	0.69			
Sr*		0.76							
I	0.33	0.40	0.42	0.89	0.82	0.87		0.22	
La	0.81	0.76	0.91	0.28	0.33	0.25	0.34		0.22
Sm	0.94	0.88	0.93	0.25	0.38	0.25			0.21
Pb	0.77	0.51	0.37						0.69
Th*		0.79			0.40				

Note that four components were identified for Skukuza and Pretoriuskop ("Pret."); the fourth component is discussed in the text. Loadings which were less than 3 times their associated standard deviation, as calculated according to *Heidam* [1982], loadings with an absolute value of less than 0.2, and negative loadings are not listed in the table.

*The elements Sr and Th were only included in the APCA for Pretoriuskop.

La, Sm, and Th) are all very highly loaded on component 1, whereas Na, Cl, and for the KNP sites also Mg and S are highly correlated with component 2. Clearly, components 1 and 2 represent soil dust and sea salt, respectively. The typical mineral dust elements all exhibit a rather high loading of about 0.4 on the sea-salt component at the highveld site, but this anomalous result is explained by the fact that this component was rather weak at Palmer (as will be seen below), so that there was some spillover from the strong to the weak component for the elements that are associated with the strong component [*Maenhaut and Cafmeyer*, 1987]. Furthermore, it should be kept in mind that a PCA is only able to resolve the aerosol components appropriately if there is sufficient variability in the data set and particularly in the relative impact of the various aerosol sources in the different samples [e.g., *Maenhaut et al.*, 1989].

Table 4 shows that the correlation of the meteorological variables with each of the two components is rather weak or insignificant. The absence of any correlation between local wind speed and component 1 (at Skukuza) strongly suggests that the airborne soil dust component is not from nearby local origin. Temperature, on the other hand, is somewhat positively correlated with component 1, and as temperature and pressure were anticorrelated with each other, pressure exhibited a negative loading on this same component. The positive correlation between temperature and the mineral dust component is likely the combined result of air mass history and of regional soil dust source strength. On hot, dry days with very low relative humidity, more soil dust is expected to become airborne on a regional scale. At the same time, there is less turbulence in the boundary layer, so that the soil dust becomes less dispersed vertically.

In the APCA for the fine fraction, 24 aerosol variables were included for Skukuza and Palmer, and 26 for Pretoriuskop. The criterion used to retain an element was the same as for the coarse fraction. Cu, As, and Sb were excluded because they gave rise to unique components (for Cu and Sb because of outliers). According to the PCA, four aerosol components were present at each of the two KNP sites, and three at Palmer. The VARIMAX rotated loadings of the various aerosol variables on the first three components are given in Table 5. Only one element (i.e., Cl) was positively correlated with component 4 (loading of 0.70 for Skukuza and of 0.92 for Pretoriuskop), but, interestingly, four elements (i.e., S, V, Zn, and Pb) exhibited negative loadings with absolute value greater than 0.3 on this component (for S the loading was about -0.5). This anticorrelation between S and Cl in this component, combined with the knowledge that the other three elements with negative loading are typically of anthropogenic origin in the fine size fraction, led us to conclude that component 4 represents a Cl loss component (perhaps mainly loss of Cl from the fine sea-salt particles), and at the

same time also a (negative) anthropogenic component, which most likely contains a major contribution from fossil fuel burning.

From an inspection of the VARIMAX rotated loadings in Table 5, it is evident that the three components represent the same three aerosol source types for the two KNP sites, but that component 3 corresponds to a different source type at Palmer than at KNP. At the lowveld, Na and Mg are highly correlated with component 3, so that it is clearly a sea-salt component there. At Palmer, on the other hand, component 3 is highly loaded with S, Se, and Pb, and to a lesser extent also with Zn, so that it seems to represent an anthropogenic (mainly fossil fuel burning) component, which corresponds partly with component 4 of the lowveld. Component 1 at all three sites has very high loadings for Al, Si, Sc, Ti, Fe, and Sm and is undoubtedly the fine fraction counterpart of the soil dust component in the coarse fraction. For component 2, black carbon (BC) and K are the elements with the highest loadings (around 0.9), whereas Rb, Br, and I have loadings between 0.7 and 0.9, and Zn of about 0.5, so that this component clearly represents biomass burning. At Palmer, Cl and Na are also highly loaded on this component, but this may be an artifact (and at the same time a limitation) of the PCA, in the sense that it was unable to separate the weak sea-salt component at this site from the biomass burning component.

The VARIMAX rotated loadings for the various components in both the coarse and the fine size fractions were converted into source profiles, absolute principal component scores (APCS) were derived for each individual sample, and the contribution from each source to the concentration of each element and of the particulate mass and BC was subsequently calculated. In this section, we will essentially restrict ourselves to presenting and discussing the contribution from the biomass burning component in the fine particle fraction. The average percentage attributions to this component are presented in Table 6 for selected aerosol variables. For the other variables included in the APCA, but not listed in Table 6, the pyrogenic component was of minor importance. As already indicated above, APCA has its inherent limitations, and, consequently, the percentage data in the table should not be treated as exact numbers. It is estimated that they have an associated uncertainty of at least 10% absolute.

Overall, the apportionments to the biomass burning component are rather similar at the three sites. Black carbon (BC), K, Rb, and I have apportionments in the range of 60-90%, and for the particulate mass (PM) and Br the data are 40-60%. Zn is attributed at a level of 40-50% to the pyrogenic component at the KNP sites, but only at a level of about 20% at Palmer. At this latter site, most of the Zn (i.e., 65%) was apportioned to the separate anthropogenic component 3. This same component was also responsible for 83% of the S and for essentially all the Se and Pb at the highveld site. The high apportionments to the pyrogenic component at Palmer for Na, Cl, and to a lesser extent for Mg and Ca are likely the result of mixing in of sea salt in the biomass burning profile. (No separate sea-salt component was identified at this site.) On the basis of the data in Table 6 it can further be concluded that biomass burning is only a minor source for the fine Ca and Mn (10-40%) and even a weaker source for Mg and S. Interestingly, most of the fine S at KNP (i.e., 50-60%) was attributed to the sea-salt component, but it was highly enriched (i.e., by a factor of 10) in this component relative to the composition of bulk seawater [*Riley and Chester*, 1971]. Most likely, this fine non-sea-salt sulfur originated from fossil fuel burning and was largely brought in to the KNP sites from over the ocean together with the sea-salt particles. As already suggested by *Annegarn et al.* [1993], polluted air masses, containing SO_2, may have been transported from the industrialized and populated areas on the highveld to over the Indian Ocean and been recirculated to the continent. During this recirculation, the SO_2 was converted to particulate sulfate, and as this sulfate was then advected within marine air, it exhibited a correlation with the sea-salt elements and became mixed in with the sea-salt component in the APCA.

Table 6. Average APCA Apportionments to the Biomass Burning Component for Selected Variables in the Fine Fraction Data Sets of the Three Fixed Sites

Variable	Skukuza	Pretoriuskop	Palmer
PM	42	60	51
BC	59	75	84
Na	5	12	87
Mg	8	8	29
S	17	24	6
Cl	0	0	100
K	57	72	86
Ca	11	29	36
Mn	15	35	16
Zn	37	47	21
Se	21	63	0
Br	35	63	65
Rb	82	77	70
I	57	64	84
Pb	10	39	0

The apportionments are expressed as percent of the mean total APCA modeled concentration.

Most of the aerosol variables presented in Table 6 were rather well modeled by the APCA. The ratios (mean APCA modeled/mean observed concentration) for the fine fraction were typically between 0.8 and 1.2 at each of the three sites. The major exceptions were Pb, with a ratio of about 0.5 at each of the two KNP sites, and Se, with a ratio of about 0.6 at Pretoriuskop and Palmer.

3.4. CMB Receptor Modeling for the Three Fixed, Ground-Based Sites

The APCA had clearly identified two components, i.e., mineral dust and sea salt, in the coarse fraction data sets, and two additional components, i.e., pyrogenic particles and anthropogenic sulfate (most likely from fossil fuel combustion), in the fine size fraction data sets. Therefore we decided to perform the CMB receptor modeling calculations with the same number of sources and with the same source types. The profiles for mineral dust and sea salt were deduced from the compositions of average crustal rock and average bulk seawater, as given by *Mason* [1966] and *Riley and Chester* [1971], respectively. The profiles for these two natural particulate sources were identical in the coarse and fine size fractions. As the profile for the fine pyrogenic particles we used the composition of the fine aerosol emitted during the flaming phase of the prescribed KNP savanna fires (i.e., the profile given in Table 3, but with upper limits replaced by

zeros). The profile from the flaming phase rather than that from the smoldering phase was selected, because aerosols from fires in savanna ecosystems are primarily derived from the flaming phase combustion phase [*Ward et al.*, 1993]. Finally, as the source profile for the fine sulfate component we used the composition of $(NH_4)_2SO_4$. The associated uncertainty (one standard deviation) for the concentrations of all variables in each of the four profiles was somewhat arbitrarily set at 10% relative. Although this 10% is probably an underestimation of the real error, trial CMB calculations with standard deviations of 30% relative indicated that the CMB apportionments changed very little.

For the CMB calculations on the coarse fraction data sets, eight elements were included in the least squares fits, i.e., Na, Mg, Al, K, Ti, V, Fe, and Sr, and apportionments were calculated for all elements that had concentrations above the detection limits. The elements Al, Ti, and Fe were chosen to serve as indicator (marker) elements for mineral dust, Na and Mg served as sea-salt indicators, and K and Sr were included as they were expected to be nearly fully attributable to the combination of both soil dust and sea salt. Si, although a typical crustal element, was not retained as an indicator element, as it is generally depleted in the mineral dust aerosol when compared to the average crustal rock composition of *Mason* [1966] (see also Figure 2a). Chlorine, the major element in sea salt, was excluded because of the possibility of some Cl loss even in the coarse size fraction (although the CMB indicated that this loss was on the average less than 30%). Apportionments to each of the two coarse components were derived for 39 aerosol variables, i.e., PM, Na, Mg, Al, Si, P, S, Cl, K, Ca, Sc, Ti, V, Cr, Mn, Fe, Co, Ni, Cu, Zn, Ga, As, Se, Br, Rb, Sr, Zr, Sb, I, Cs, Ba, La, Ce, Sm, Eu, Lu, Au, Pb, and Th. Of these 39 variables, 29 were essentially fully attributed to the mineral dust source; the exceptions were PM, Na, Mg, S, Cl, K, Ca, Se, Sr, and I. The average apportionment of Na to sea salt, in percent of the mean total CMB-predicted atmospheric concentration, was 84% for Skukuza, 73% for Pretoriuskop, but only 12% for the highveld. For the particulate mass (PM), the corresponding percentages were 32%, 20%, and 1.3%, respectively. The halogens Cl and Br were at all three sites attributed at a level of 90% or more to the sea-salt component. For S, more than 95% was on the average apportioned to this same component at the two KNP sites, but only about 60% at Palmer.

The CMB predicted the observed atmospheric concentrations for the coarse fraction quite well for the eight elements that were included in the least squares fits. For example, at the Pretoriuskop site, the mean (total CMB-predicted/observed) concentration ratios, when averaged over all 40 samples, were between 0.75 and 1.3 for the eight marker elements, and the associated percentage standard deviations remained limited to about 10-20%. Also most of the other elements were predicted rather well by the CMB. In fact, of the 39 elements for which apportionments were calculated, 28 had mean (total CMB-predicted/observed) concentration ratios between 0.5 and 2.0 at each of the three sites. Cr and Br also exhibited ratios within the 0.5-2.0 range for the two KNP sites, but they were clearly underpredicted at Palmer, where the mean ratios were about 0.2 for both elements. According to *Kowalczyk et al.* [1978], when the discrepancy between the total modeled and observed elemental concentrations remains less than a factor of 2, the CMB apportionment can be considered acceptable. This should particularly be so for the elements attributed to the mineral dust source, since the composition of the regional mineral dust aerosol which is generated from the southern African soils may differ substantially from that of Mason's average crustal rock.

The mean (total CMB-predicted/observed) concentration ratios for the particulate mass (PM) were 0.71±0.07 (N=41), 0.73±0.06 (N=40), and 0.77±0.13 (N=42) for Skukuza, Pretoriuskop, and Palmer, respectively, thus indicating that PM was systematically underpredicted by about 20-30%. There are various possible explanations for this "missing" coarse particle mass. To some extent, it may have been caused by the use of Mason's average crustal rock composition as the mineral dust profile and by the choice of indicator elements. Part of the missing mass may have been water (the weighings were done in Gent at 50% relative humidity); very likely, organics made up a substantial fraction of it, and major inorganic compounds that were not measured by us (e.g., nitrate) may also have contributed. Also non-sea-salt and noncrustal sulfate contributed a little, but the calculations showed that this sulfate (if present as $(NH_4)_2SO_4$) was only responsible for about 15% of the missing mass. On the basis of NO_3^- and SO_4^{2-} data for the coarse fraction of background samples from regional flights (M. O. Andreae et al., Airborne studies of emissions from savanna fires in southern Africa, 2, Aerosol chemical composition, manuscript in preparation, 1996), it is estimated that nitrate (as NH_4NO_3) represents another 15% of the missing mass. The contribution from biomass burning products should also not be excluded, but must have been minor. Indeed, the percentage missing mass varied little from sample to sample, whereas the APCA and CMB on the fine fraction data indicated that there was a very large sample-to-sample variability in the impact from the pyrogenic emissions. Furthermore, most of the elements that are present in the "pure" pyrogenic coarse aerosol (see Table 3 and the discussion in section 3.2) were predicted within a factor of 2 by our two-source CMB calculations. This was so for P, Cl, K, Ca, Mn, and Sr, and four of these six elements (Cl, K, Ca, Sr) were in fact even overpredicted.

The nine elements for which the CMB-predicted and observed concentrations in the coarse fraction differed by more than a factor of 2 were S, Cu, Zn, As, Se, Sb, I, Au, and Pb. All these elements were underpredicted, suggesting that they did not mainly originate from mineral dust and sea salt, but instead from other sources. For S at the two KNP sites, and for Cu, Zn, and As at all three sites, the mean (total CMB-predicted/observed) concentration ratios were still in the range of 0.2-0.4, but S at Palmer and Se, Sb, I, Au, and Pb at the three sites were underpredicted by a factor of 20 or more. Most likely, the coarse S, Cu, As, Se, Sb, and Pb are mainly attributable to emissions from fossil fuel burning and various high-temperature industrial processes. (Note that all these elements, except Cu, exhibited fine/coarse ratios of 1 or higher.) For Zn and I, pyrogenic emissions may have been the most important contributors.

For the fine fraction CMB calculations, eight species were included in the least squares fits, i.e., BC, Na, Mg, Al, S, K, Ti, and Fe. The elements Al, Ti, and Fe were indicators for the mineral dust source, Na and Mg served as sea-salt indi-

Table 7. Average CMB Apportionments to Four Particle Sources for the Fine Fraction Data Sets of the Three Fixed Sites

	Mineral Dust			Sea Salt			Biomass Burning			Sulfate			Mean (Predicted/
Variable	Skukuza	Pret.	Palmer	Skukuza	Pret.	Palmer	Skukuza	Pret.	Palmer	Skukuza	Pret.	Palmer	Observed)
PM	13	19	22	16	11	1.6	39	38	41	33	33	36	0.98
BC*							100	100	100				0.95
Na*	7	14	50	91	84	41	2	3	9				1.02
Mg*	31	50	88	69	50	12							0.91
Al*	99	99	99	0	0	0	0.8	0.6	0.5				1.19
S*	0	0.1	0.1	5	3	0.5	3	3	3	93	94	97	1.00
Cl	0	0	0.1	73	64	21	27	36	79				26
K*	15	21	24	8	5	0.8	77	74	75				0.99
Ca	70	83	96	28	15	2	1.8	1.4	1.5				1.80
Mn	95	97	97	0	0	0	5	3	3				0.77
Fe*	99	99	99	0	0	0	1	0.7	0.6				1.06
Cu	44	54	56	0.1	0	0	56	46	44				0.31
Zn	6	8	9	0	0	0	94	92	91				0.61
Br	0.1	0.1	0.2	54	45	11	46	55	89				0.65
Rb	45	55	58	2	1	0.2	53	44	42				0.62
Sr	56	74	95	44	26	5							1.28
Sb	5	7	8	0.2	0.2	0	95	93	92				0.13
I	0.2	0.3	0.3	0.7	0.5	0.1	99	99	99				0.15
Cs	38	48	50	0.2	0.1	0	62	52	50				0.21
Pb	16	22	24	0	0	0	84	78	76				0.03

The apportionments are expressed as percent of the mean total CMB-predicted concentration. Comparison of total CMB-predicted with observed concentrations is given for Skukuza. Blank entries in the table indicate that the element was not present in the source profile. A value of zero means that the percentage apportionment was smaller than 0.5%. The following elements were at all three sites for 100% attributed to the mineral dust source, and their mean (total predicted/observed) concentration ratios for Skukuza are given in parentheses: Si (1.89), Sc (1.38), Ti (0.77), V (0.39), Co (0.40), La (0.49), Sm (0.62), Th (0.25). "Pret." denotes Pretoriuskop.

*Variables which were included in the least squares fits.

cators, BC and K were marker elements for the biomass burning source, and S the marker for the ammonium sulfate component. Apportionments to each of the four fine components were derived for 30 aerosol variables, i.e., PM, BC, Na, Mg, Al, Si, S, Cl, K, Ca, Sc, Ti, V, Mn, Fe, Co, Cu, Zn, As, Se, Br, Rb, Sr, Sb, I, Cs, La, Sm, Pb, and Th. The average apportionments and mean (total CMB-predicted/observed) concentration ratios for 28 of these variables are given in Table 7. The predicted/observed ratios are only presented for the Skukuza site, but they were quite similar at the other two sites. As and Se, the two elements for which the data are not given in Table 7, were very poorly predicted by the CMB (As was underpredicted by a factor of about 30, Se by a factor of more than 1000), but, then, these two elements were only present in the mineral dust and sea-salt profiles (unfortunately, As and Se were below the detection limit in most of the SFU samples from near the prescribed fires, so that their concentrations were set equal to zero in the pyrogenic profile).

Of the 28 variables of Table 7, 10 were essentially fully attributed to the mineral dust source, and for Mn the mean apportionment to that source was 95% or more. The observed concentrations of these various "crustal" elements were all predicted within a factor of 2, with the exception of Th (and for Skukuza also V and Co). The underprediction for V points to an additional source for this element, which most likely is the burning of residual oil. At the two KNP sites, sea salt appears to be the major source for fine Na and Cl and also an important source for some other elements (Mg, Br, Sr). The fact that the observed Cl is very largely overpredicted by the CMB confirms that major losses of fine Cl did indeed occur (in the atmosphere, on the filter during sampling, and/or in between sampling and analysis). The pyrogenic component is the dominant contributor to the CMB-predicted concentrations of BC, K, Zn, Sb, I, and Pb, and it appears also to be a major source for PM, Cl, Cu, Br, and Cs. Several of these variables are very well or rather well predicted by the CMB model, but others are clearly underpredicted. The latter is the case for Cu, and in particular for Sb, I, Cs, and Pb. For I, the concentration in our pyrogenic profile may well be too low, as a large fraction of this element is most likely still in the vapor phase at the time of emission and only becomes converted to (or associated with) the particulate phase during the atmospheric transport. For the same reason, the fraction of S attributed to the pyrogenic component may be an underestimate of the true pyrogenic particulate S at the fixed sites. It should be mentioned in this context, however, that the APCA also indicated that biomass burning contributed rather little to the regional airborne S. For I, on the other hand, the average APCA apportionment to the pyrogenic component was in the range of 60-80%.

That the observed concentrations of Sb and Pb are very poorly predicted by the CMB strongly suggests that these two elements did not originate from the four included sources (note, though, that pure ammonium sulfate was used for the sulfate profile). Similarly as for the coarse fraction, Sb and Pb are also in the fine fraction probably mainly attributable to fossil fuel burning and various high-temperature industrial processes. These same sources were also likely the

prevailing sources for the fine As and Se, and for the fine Cu (and perhaps also Zn) that was not explained by the four-source CMB.

A very important finding from Table 7 is that about 40% of the fine particulate mass (PM) is attributed to the pyrogenic particles, and about one third to the sulfate component. Moreover, the observed PM levels were surprisingly well predicted by the four-source CMB. Indeed, the mean (total CMB-predicted/observed) concentration ratios for the fine PM were 0.98±0.14 (N=41), 1.00±0.21 (N=40), and 0.80±0.14 (N=42) for Skukuza, Pretoriuskop, and Palmer, respectively.

CMB and APCA are two widely different receptor modeling approaches, and it is generally believed that CMB gives the better results, but it has the disadvantage that the important aerosol sources must be known and that the profiles for these sources must be reasonably accurate. It is very comforting to notice that the two approaches gave rather similar apportionments for the various data sets. The similarity in average attributions to the biomass burning component can be judged by comparing the data in Tables 6 and 7. Considering that the error of the APCA apportionments has been estimated to be at least 10% absolute, the APCA and CMB biomass burning attributions for PM are fully consistent; BC, K, Rb, and I are in both approaches predominantly (for 60-100%) apportioned to the pyrogenic component, but this component is of minor importance for S, Ca, and Mn. Furthermore, the APCA and CMB results showed rather good similarity not only on an average basis, but also for the individual samples. In fact, the sample-to-sample variability

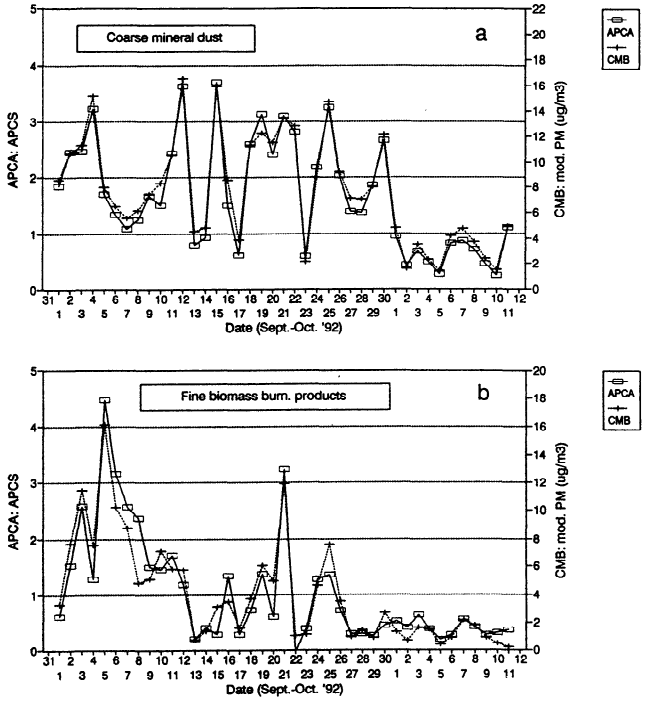

Figure 7. Comparison of absolute principal component scores (APCS) from the APCA on the Skukuza data set with particle mass attributions derived from the CMB (a) for the soil dust component in the coarse particle size fraction and (b) for the biomass burning component in the fine size fraction.

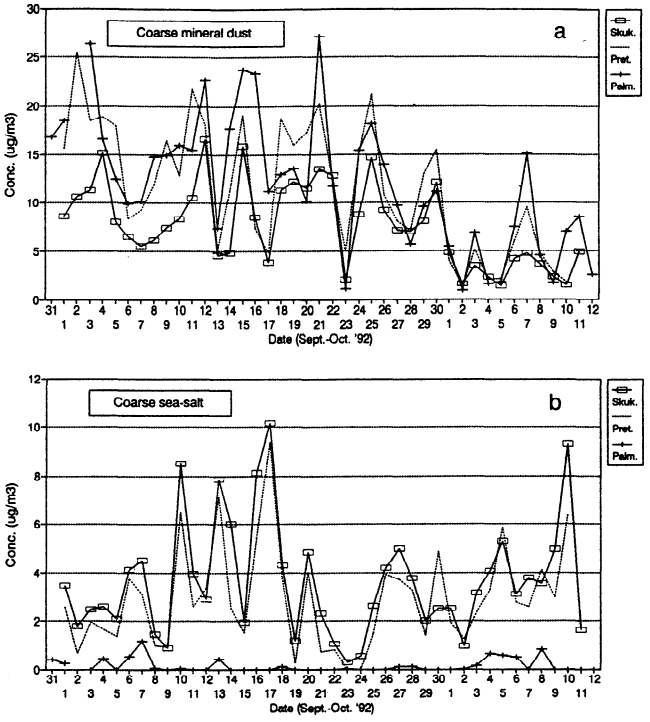

Figure 8. Time trends for the coarse particle mass (PM) apportioned (a) to mineral dust and (b) to sea salt for the SFU samples from Skukuza, Pretoriuskop, and Palmer.

in the attribution to a particular component was often surprisingly similar in both approaches. This is illustrated in Figure 7, where the APCS from the APCA on the Skukuza data set are compared with particle mass attributions derived from the CMB. (The APCS are a measure for the intensity (importance) of a component in the individual samples.) Figure 7a presents the comparison for the soil dust component in the coarse particle size fraction, whereas Figure 7b shows the results for the biomass burning component in the fine size fraction.

3.5. Time Trends of the Aerosol Components and Relation to Meteorology and Atmospheric Circulation

We already indicated in section 3.1 that there was a good similarity in the time trends of many particulate species (elements) at the three fixed sites, and in particular for the two lowveld sites Skukuza and Pretoriuskop. Rather than dealing with the many individual species, we prefer to discuss in this section the time trends of the major aerosol components, as identified by the APCA and apportioned by the CMB. In fact, we will restrict our discussion to the atmospheric particle mass (PM) concentrations that were attributed by the CMB to the major aerosol components. The time trends for the coarse PM apportioned to mineral dust and to sea salt are shown in Figure 8, and those for fine PM attributed to biomass burning and to sulfate are presented in Figure 9. The time trends for fine PM from mineral dust and sea salt are not shown, but they were quite similar to their coarse fraction counterparts. The very good correlation between the time trends of the two lowveld sites and the close similarity in atmospheric concentrations (particularly for sea salt, bio-

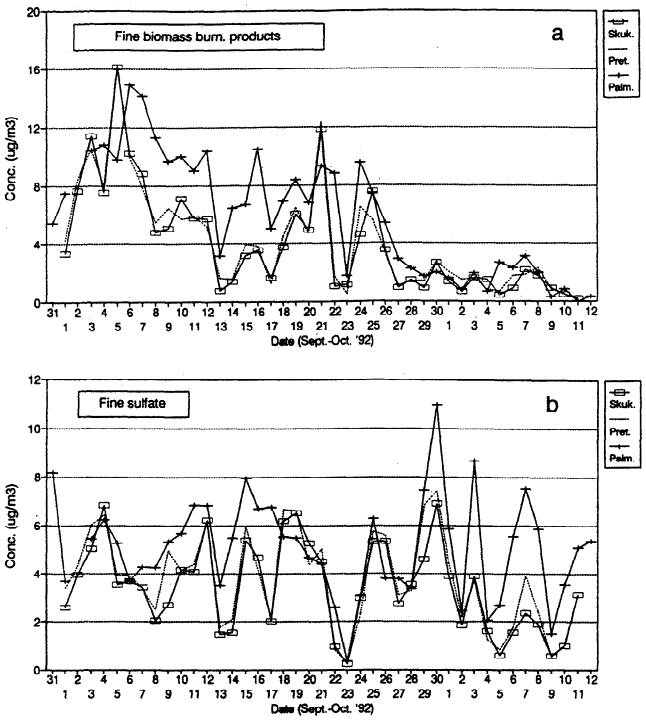

Figure 9. Time trends for the fine particle mass (PM) apportioned (a) to biomass burning and (b) to sulfate for the SFU samples from Skukuza, Pretoriuskop, and Palmer.

mass burning products, and sulfate) indicate that we did not collect particulate materials (e.g., pyrogenic aerosols) from a nearby, very local origin, but instead that the samples were regionally representative. Furthermore, the coherence between the data from the two lowveld sites with those from the highveld site suggests that the boundary layer air compositions of the lowveld and the highveld were to some extent coupled by mesoscale meteorology and atmospheric circulation. However, this coupling was clearly only partial, since the sea-salt component exhibited a much lower intensity at Palmer than at the two KNP sites (see Figure 8b).

According to South African Weather Bureau data and analyses, the major feature during the month of September was a cold period over the entire country from September 21 to 23. On September 21 a low developed over the interior of South Africa; this low was accompanied by a strong cold front which moved from south to north and passed through the eastern Transvaal on September 22; behind this front came an Atlantic high which gave rise to cold weather on September 22 and 23. Furthermore, the strong winds which preceded the cold front caused serious veld and bush fires in the eastern and southeastern Transvaal (G. R. Vallance, Weerbureau Nuusbrief, South African Weather Bureau, September 1992). The average daily temperatures recorded on September 23 at our three fixed sampling sites were the lowest of our entire 45-day sampling period (at Skukuza, only 15.6°C on September 23, whereas the overall average for the entire period was 23.4°C). At the same time, the average daily wind speed at Skukuza was higher on September 22-23 than on all other days. Most likely, vertical mixing was also more pronounced on these same two days. Passages of cold fronts through the eastern Transvaal also occurred on several other days, i.e., on September 6, 14, and 17 and on October 2 and 9. By relating these observations with the time trends of coarse and fine PM (Figure 4), it is seen that the cold front passages generally gave rise to much decreased PM concentrations. In fact, the lowest coarse PM levels were noted on September 23 and October 2, whereas the fine PM levels at the two KNP sites were low on all front passages, except for that of September 6. Moreover, the fronts led not only to decreased PM levels, but often also to low concentrations for each of the CMB-apportioned components (Figures 8 and 9). This is particularly evident for September 23, when the strong cold front passed through the study area, but for the KNP sites we also observed clear minima in the levels of coarse mineral dust (Figure 8a) and of fine pyrogenic products and sulfate (Figure 9) on all other front passages, except on September 6.

Further clues for explaining the observed time trends of coarse and fine PM and in particular of the various aerosol components (Figures 8 and 9) were obtained from 10-day, three-dimensional backward trajectories for the Kruger National Park region [*Källberg*, 1984; *Garstang et al.*, this issue]. These trajectories were calculated for an arrival time of 1200 UT each day and for five arrival levels, i.e., 900, 850, 800, 700, and 500 hPa. As the average pressures at Skukuza and Pretoriuskop were 984 and 944 hPa, respectively, during our sampling period, the trajectories with the two lowest arrival levels (900 and 850 hPa) were thought to be the most appropriate ones for interpreting the observed atmospheric concentrations at the two KNP sites. For the highveld site (average pressure 786 hPa) the trajectories arriving at 700 hPa were used. With only few exceptions, the 900-hPa trajectories had a very clear maritime character during our 45-day sampling period. The maritime air masses came in from the east (the Indian Ocean), but very often the trajectories then curved southward and subsequently westward well below southern Africa to have their endpoint (10 days backward in time) over the South Atlantic Ocean and occasionally even over the Antarctic Ocean. The trajectories at 850 hPa usually exhibited rather similar characteristics as those at 900 hPa, except during the first week of our sampling period (August 30 to September 6), when they were of continental nature instead. As to the 700-hPa back trajectories, these were almost exclusively continental in character and they remained generally confined to the southern African continent, thereby often showing extensive recirculation, but occasionally they extended back to over the mid-Atlantic west of Africa.

The general contrast in air mass origin between the 700-hPa arrival level and the 900- and 850-hPa arrival levels is fully consistent with our observations that the sea-salt component is virtually absent at Palmer, whereas it is at times very important at the two lowveld sites (Figure 8b). As to the differences between the 900- and 850-hPa trajectories (maritime versus continental) in the first week of our sampling campaign, the overall low intensity of the sea-salt component at KNP during that time seems to suggest that the 850-hPa trajectories more accurately describe the air mass transport to the Kruger National Park region. On the other hand, it should be indicated that the relationship between the intensity of the sea-salt component and the origin of the air mass is not always straightforward. While the elevated sea-salt concentrations at the two KNP sites (Figure 8b) were

observed on days when direct air mass transport from over the Indian Ocean took place for both the 900- and 850-hPa arrival levels (this was so on September 7, 10, 13, 14, 16, 17, 26, 27, and 28 and on October 4, 5, 9, and 10; as an example, the trajectories for September 17 are shown in Figure 10a), the direct influx of maritime air on some other days (September 23 (trajectories in Figure 10b), September 24, October 2) did not lead to noticeable sea-salt aerosol levels. Incidentally, two of these three days with maritime air influx and low sea salt were also days when a cold front passed through the area.

From an inspection of the time trends for the biomass burning component in the fine fraction (Figure 9a) it is evident that this component was quite important at all three fixed sites during the period September 2-12, then again on September 19-21, and finally on September 24-25. Furthermore, within these episodes one observes pronounced peak levels at the two KNP sites on September 5 and 21. From September 27 onward the pyrogenic component is very low at all three sites. The general trend of decreasing levels of biomass burning products from late August to mid-October is consistent with the overall decrease in fire activity in southern Africa as the dry season progresses [*Cahoon et al.*, 1992]. But this trend is reinforced here by the changes in atmospheric circulation and air mass origin with time. Indeed, during the major episode of pyrogenic influence (September 2-12), the air masses at the 850-, 800-, and 700-hPa arrival levels were essentially all of continental nature. Furthermore, the trajectories (those for September 5 are shown in Figure 10c) indicated that extensive recirculation had taken place over the continent and that the air masses had remained confined to the latitude band between 10° and 27°S during the 10 days prior to arrival. During its passage the air likely picked up pyrogenic products from several countries (e.g., Angola, Zambia, Zimbabwe, Mozambique) to the north and northeast of South Africa, where the fire activities are generally more intense than in South Africa itself [e.g., *Cahoon et al.*, 1992; *Andreae*, 1993a]. On September 7, the air masses for the three lowest levels (900, 850, and 800 hPa) had clearly originated over the Indian Ocean, but they then came in from a northeasterly direction and spent the last 24-48 hours prior to their arrival over Mozambique. The air masses for 900 and 850 hPa on September 10 were also of marine origin, but they came in again from the northeast.

After the first pyrogenic period, the air masses for 900 and 850 hPa were during several days (September 13-17) consistently of marine origin and came in from the south to southeast. This resulted in much lower levels of the pyrogenic component and gave rise to increased sea-salt concentrations at the two KNP sites, as indicated above. During the second, short, pyrogenic episode (September 19-21), the air masses were first clearly continental, with very extensive recirculation within the 20°-30°S latitude band, but on September 21 the air (for the 900- and 850-hPa levels; see Figure 10d) had originated over the mid-Atlantic, passed around the south African continent and over the Indian Ocean, and then came in above the African continent over Mozambique and Zimbabwe to enter South Africa from the northeast, much in the same way as on September 7. This latter segment of the trajectory could have brought in pyrogenic materials. On the other hand, it is quite likely that biomass burning products from the serious veld and bush fires that occurred in the eastern Transvaal just before the strong cold front (see above) were also advected to the sampling sites.

During the last, brief, pyrogenic peak period (September 24-25) the air at the three lowest levels (900, 850, and 800 hPa) was ultimately of oceanic origin, but the trajectories passed north of the KNP area to curve then to the south and west, so that the air came finally to the sampling sites from the west (this was particularly evident on September 25; see Figure 10e). From about September 27 until October 11 (the last day of our samplings at the KNP sites), the air masses were generally of direct maritime origin for each of the three lowest arrival levels; the air came in over the continent from the southeast, but the trajectories had their endpoints above the southern Atlantic and occasionally even further south (i.e., over the Antarctic Ocean). On September 30, and to a lesser extent also on October 7, the trajectories passed north and west of the KNP area prior to their arrival (much in the same way as on September 25), and interestingly, small local maxima in the biomass component were observed on those two days.

The time trends for the sulfate component in the fine fraction (Figure 9b) show a pattern which is overall quite different from that for the pyrogenic component (Figure 9a). Occasionally, the two components have high levels on the same day (i.e., on September 12, 19, and 25). But the pyrogenic component shows a clear tendency to decrease with time over our 45-day sampling period, whereas the sulfate component actually exhibits several maxima during the last third of this period, with the peak sulfate level for all three sites being observed on September 30. At first sight, there appears to be some resemblance between the trends for fine sulfate and those for coarse sea salt (Figure 8b). Furthermore, fine sulfate shows elevated levels in the period from September 12 to September 21 and then again from September 25 onward, that is, during periods when the air for the three lowest arrival levels (900, 850, and 800 hPa) was generally of maritime origin. However, a close comparison of Figures 8b and 9b actually indicates that the sulfate and sea-salt component are in general anticorrelated with each other during these two "maritime" periods.

Overall, the variability in the sulfate component resembles much more closely that of the mineral dust component (Figure 8a) than that of any other component, in the sense that sulfate and mineral dust usually exhibit maxima (and also minima) on the same days, although the variation in the intensity of these maxima is rather different for the two components. This coherence between sulfate and mineral dust clearly points to a continental origin for the sulfate. Furthermore, the sulfate component is often significantly more elevated at Palmer than at the two KNP sites; this is particularly true for the peak sulfate days of the last third of the sampling period (i.e., on September 30 and October 3 and 7). Considering that the 700-hPa air mass trajectories (thought to be most representative for air mass transport to the highveld site) had a much more continental character than the trajectories for the lower arrival levels, which were very often of maritime nature, the continental origin of the sulfate becomes even more plausible. For example, the air mass arriving at the 700-hPa level on September 30 (see Figure 10f) had already spent 7 days over the continent prior to its arrival,

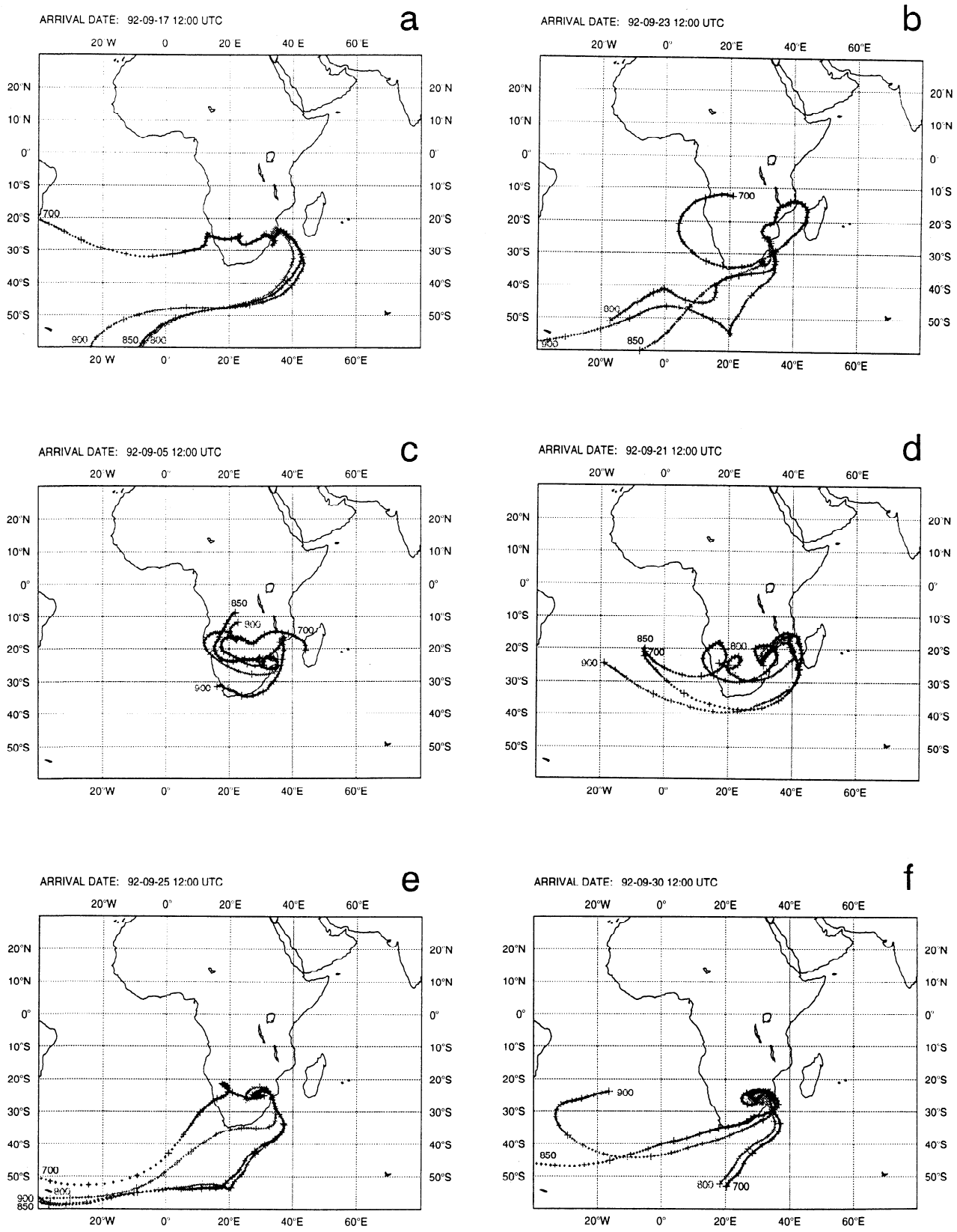

Figure 10. Ten-day, three-dimensional air mass back trajectories for four different arrival levels at the Kruger National Park. The arrival level is indicated near the start for each type of trajectory. The pluses on each trajectory give the position of the air mass at 24-hour intervals.

whereas that for the 850-hPa level was only over the continent for 2 days. As to the actual sources for the SO_2 precursor gas of the fine sulfate, the major contribution most likely comes from fossil fuel (i.e., coal) burning and various industrial activities which take place on the Transvaal highveld around and to the east of the Johannesburg-Pretoria area.

4. Summary and Conclusions

Size-fractionated aerosol samples were collected at three fixed sites and near a number of prescribed savanna fires, and analyzed for up to 49 species (elements). From a comparison of the size distributions and the crustal enrichment factors for the pyrogenic samples with those for the samples from the fixed "background" sites, it can be concluded that savanna fires are a major source for the following species (elements) in the coarse size fraction: PM, BC, P, K, Ca, Mn, Zn, Sr, and I; and this is the case in both the flaming and smoldering phases. In the fine fraction, both fire phases are a major source for PM, BC, the halogens (Cl, Br, I), K, Cu, Zn, Rb, Sb, Cs, and Pb; the flaming phase is also a prominent source of Na and S. Furthermore, the flaming phase of the savanna fires appeared to be an efficient mobilizer of coarse soil dust into the atmosphere.

The data sets from the three fixed sites (which included up to forty-two 24-hour samples per site) were subjected to multivariate (APCA) and CMB receptor modeling in order to identify the major aerosol source types (components) and to apportion the particulate mass and the various elements to these components. APCA indicated that the coarse fraction data sets contained only two dominant components, i.e., mineral dust and sea salt, and that two additional components, i.e., pyrogenic particles and anthropogenic sulfate (most likely from fossil fuel burning) were present in the fine fraction. The mineral dust and sea-salt components showed only a rather weak or insignificant correlation with local wind speed, temperature, or pressure. The fact that the mineral dust component was not correlated with local wind speed strongly suggests that the airborne soil dust was not of nearby local origin.

The two-component CMB apportionments for the coarse fraction data sets indicated that on the average, the mineral dust component was the major contributor to the coarse particulate mass. The average apportionment of PM to mineral dust, in percent of the mean total CMB-predicted atmospheric PM concentration, was 68% for Skukuza, 80% for Pretoriuskop, and 98.7% for the highveld, with the remaining 32%, 20%, and 1.3% for each of these sites thus being attributed to sea salt. However, the two-component CMB model systematically underpredicted the observed PM concentration by about 20-30%. Various explanations are possible for this "missing" coarse particle mass. Part of it may have been water; very likely, organics made up a substantial fraction of it, and it was estimated that excess sulfate (i.e., non-sea-salt and noncrustal sulfate) and nitrate may each have been responsible for about 15% of the missing mass. The contribution from biomass burning products should also not be excluded, but must have been minor, as several elements that are present in the "pure" pyrogenic coarse aerosol (i.e., Cl, K, Ca, Sr) were already overpredicted by the two-component CMB.

From the four-component CMB apportionments for the fine fraction data sets it appeared that the pyrogenic component was the dominant contributor to the concentrations of BC, K, Zn, and I, and a major source for PM, Cl, Cu, Br, and Cs. A very important finding was that about 40% of the fine particulate mass (PM) was attributed to the pyrogenic particles and about one third of it to the sulfate component. Moreover, the total CMB-predicted PM levels agreed extremely well with the observed PM concentrations (particularly at the two KNP sites).

The fine fraction APCA and CMB attributions to biomass burning were rather similar to each other: For PM the apportionments were entirely consistent; BC, K, Rb, and I were in both approaches predominantly (for 60-100%) apportioned to the pyrogenic component, but this component was of minor importance for S, Ca, and Mn.

The atmospheric concentrations of the particulate mass, the CMB-apportioned components, and many elements exhibited a very similar sample-to-sample variability at the three fixed sites. The correlation between the time trends was particularly good for the two lowveld (KNP) sites, and, moreover, at these sites there was also a close similarity in the actual atmospheric concentrations of the apportioned components (particularly for sea salt, biomass burning products, and sulfate). This all indicates that we did not collect particulate materials (e.g., pyrogenic aerosols) of nearby, very local origin, but instead that the samples were regionally representative. Furthermore, the coherence between the data from the two lowveld sites with those from the highveld site suggested that the boundary layer air compositions of the lowveld and the highveld were to some extent coupled by mesoscale meteorology and atmospheric circulation. By relating the time trends of the coarse and fine PM to meteorological observations it was found that cold front passages generally gave rise to much decreased PM concentrations. The frontal passages also often led to minima in the trends for the CMB-apportioned components. This was particularly evident for September 23, when a very strong cold front passed through the study area.

Very useful information on the source regions of the various aerosol components was obtained by relating the time trends of the components to 10-day, three-dimensional air mass trajectories. To evaluate the air mass transport to the KNP area, we used trajectories with arrival levels of 900 and 850 hPa, but the latter ones seemed to describe the transport more accurately. For the transport to the highveld site (with average pressure of 786 hPa), trajectories arriving at 700 hPa were used. As expected, elevated levels of the sea-salt component at the two lowveld sites were observed when direct air mass transport from the Indian Ocean took place for both the 900- and 850-hPa arrival levels. Whereas such maritime transport occurred rather regularly for the lowest arrival levels, the 700-hPa trajectories were almost exclusively continental in character and remained generally confined to the southern African continent. As a consequence, the sea-salt component was virtually absent at Palmer.

The biomass burning component in the fine size fraction showed a general decrease from late August to mid-October at all three fixed sites, which is consistent with the overall decrease in fire activity in southern Africa as the dry season comes to its end [*Cahoon et al.*, 1992]. But this trend was reinforced here by the changes in atmospheric circulation and air mass origin with time. Indeed, during the episodes of pyrogenic influence, most of the air mass trajectories were of continental nature, showed extensive recirculation, and

remained confined to the latitude band between 10° and 30°S, so that pyrogenic products were likely picked up from several countries (e.g., Angola, Zambia, Zimbabwe, Mozambique) to the north and northeast of South Africa, where the fire activities are generally more intense than in South Africa itself [e.g., *Cahoon et al.*, 1992; *Andreae*, 1993a]. On some days with elevated pyrogenic levels, the air masses had clearly originated over the ocean instead of over the continent, but then came in from a northeasterly direction, and spent the last 24-48 hours prior to their arrival over Mozambique.

The time trends for the sulfate component in the fine fraction exhibited a pattern which was quite different from that for the pyrogenic component, and overall they showed more resemblance to the time trends of the mineral dust than to those of any other component, thus suggesting that the sulfate was of continental origin. Also, the sulfate component was often significantly more elevated at the highveld site than at the two lowveld sites (this was particularly true for the peak sulfate days of the last third of the sampling period). It was concluded that the major contribution to this sulfate most likely came from fossil fuel (i.e., coal) burning and various industrial activities which take place on the Transvaal highveld around and to the east of the Johannesburg-Pretoria area.

Acknowledgments. This work was funded under contract GC/02/001 by the Impulse Programme "Global Change", which is supported by the Belgian State – Prime Minister's Service - Federal Office for Scientific, Technical and Cultural Affairs. Partial financial assistance was also provided by the Belgian "Nationaal Fonds voor Wetenschappelijk Onderzoek" and the "Interuniversitair Instituut voor Kernwetenschappen". A.L.F. Potgieter provided invaluable logistical support during the field work. The assistance of J. Sanders, B. Du Preez and E. Du Preez in the sample collections is acknowledged. C. Gilot assisted in the chemical analyses. We are grateful to N. Zambatis for providing the reports of the South African Weather Bureau, to S. Piketh for various informations on the sampling sites, and to R. Swap and P. Kållberg for the air mass trajectories.

References

Andreae, M. O., Soot carbon and excess fine potassium: Long-range transport of combustion derived aerosols, *Science, 220*, 1148-1151, 1983.

Andreae, M. O., Global distribution of fires seen from space, *Eos Trans. AGU, 74*, 129, 1993a.

Andreae, M. O., The influence of tropical biomass burning on climate and the atmospheric environment, in *Biogeochemistry of Global Change: Radiatively Active Trace Gases*, edited by R. S. Oremland, pp. 113-150, Chapman and Hall, New York, 1993b.

Andreae, M. O., T. W. Andreae, R. J. Ferek, and H. Raemdonck, Long-range transport of soot carbon in the marine atmosphere, *Sci. Total Environ., 36*, 73-80, 1984.

Annegarn, H. J., M. A. Kneen, S. J. Piketh, A. J. Horne, H. S. P. Hlapolosa, and G. A. Kirkman, Evidence for large-scale circulation of anthropogenic sulphur over South Africa, paper presented at the National Association for Clean Air Conference, Brits, South Africa, November 11-13, 1993.

Arimoto, R., R. A. Duce, B. J. Ray, A. D. Hewitt, and J. Williams, Trace elements in the atmosphere in American Samoa: Concentrations and deposition to the tropical South Pacific, *J. Geophys. Res., 92*, 8465-8479, 1987.

Artaxo, P., H. Storms, F. Bruynseels, R. Van Grieken, and W. Maenhaut, Composition and sources of aerosols from the Amazon Basin, *J. Geophys. Res., 93*, 1605-1615, 1988.

Artaxo, P., M.A. Yamasoe, J.V. Martins, S. Kocinas, S. Carvalho, and W. Maenhaut, Case study of atmospheric aerosol measurements in Brazil: Aerosol emissions from Amazon Basin fires, in *Fire in the Environment: The Ecological, Atmospheric and Climatic Importance of Vegetation Fires*, edited by P. J. Crutzen and J. G. Goldammer, pp. 139-158, John Wiley, New York, 1993.

Bauman, S., P. D. Houmere, and J. W. Nelson, Cascade impactor aerosol samples for PIXE and PESA analysis, *Nucl. Instrum. Methods, 181*, 499-502, 1981.

Cachier, H., J. Ducret, M. P. Brémond, V. Yoboué, J.-P. Lacaux, A. Gaudichet, and J. Baudet, Biomass burning aerosols in a savanna region of the Ivory Coast, in *Global Biomass Burning: Atmospheric, Climatic, and Biospheric Implications*, edited by J. S. Levine, pp. 174-180, MIT Press, Cambridge, Mass., 1991.

Cahill, T. A., L. L. Asbaugh, J. B. Barone, R. Eldred, P. J. Feeney, R. G. Flocchini, C. Goodart, D. J. Shadoan, and G. Wolfe, Analysis of respirable fractions in atmospheric particles via sequential filtration, *J. Air Pollut. Control Assoc., 27*, 675-678, 1977.

Cahoon, D. R., Jr, B. J. Stocks, J. S. Levine, W. R. Cofer III, and K. P. O'Neill, Seasonal distribution of African savanna fires, *Nature, 359*, 812-815, 1992.

Charlson, R. J., J. Langner, H. Rodhe, C. B. Leovy, and S. G. Warren, Perturbation of the northern hemisphere radiative balance by backscattering from anthropogenic sulfate aerosols, *Tellus, 43B*, 152-163, 1991.

Charlson, R. J., S. E. Schwartz, J. M. Hales, R. D. Cess, J. A. Coakley, Jr., J. E. Hansen, and D. J. Hofmann, Climate forcing by anthropogenic aerosols, *Science, 225*, 423-430, 1992.

Crutzen, P. J., and M. O. Andreae, Biomass burning in the tropics: Impact on atmospheric chemistry and biogeochemical cycles, *Science, 250*, 1669-1678, 1990.

Crutzen, P. J., and J. G. Goldammer (Eds.), *Fire in the Environment: The Ecological, Atmospheric and Climatic Importance of Vegetation Fires*, John Wiley, New York, 1993.

Dickinson, R. E., Effect of fires on global radiation budget through aerosol and cloud properties, in *Fire in the Environment: The Ecological, Atmospheric and Climatic Importance of Vegetation Fires*, edited by P. J. Crutzen and J. G. Goldammer, pp. 107-122, John Wiley, New York, 1993.

Garstang, M., P. D. Tyson, R. Swap, M. Edwards, P. Kållberg, and J. A. Lindesay, Horizontal and vertical transport of air over southern Africa, *J. Geophys. Res.*, this issue.

Gaudichet, A., F. Echalar, B. Chatenet, J.P. Quisefit, G. Malingre, H. Cachier, P. Buat-Ménard, P. Artaxo, and W. Maenhaut, Trace elements in tropical African savanna biomass burning aerosols, *J. Atmos. Chem., 22*, 19-39, 1995.

Gordon, G. E., Receptor models, *Environ. Sci. Technol., 22*, 1132-1142, 1988.

Heidam, N. Z., Review: Aerosol fractionation by sequential filtration with Nuclepore filters, *Atmos. Environ., 15*, 891-904, 1981.

Heidam, N. Z., Atmospheric aerosol factor models, mass and missing data, *Atmos. Environ., 16*, 1923-1931, 1982.

Henry, R. C., C. W. Lewis, P. K. Hopke, and H. J. Williamson, Review of receptor model fundamentals, *Atmos. Environ., 18*, 1507-1515, 1984.

John, W., S. Hering, G. Reischl, and G. Sasaki, Characteristics of Nuclepore filters with large pore sizes, II, Filtration properties, *Atmos. Environ., 17*, 373-382, 1983.

Kållberg, P., Air parcel trajectories from analysed or forecast windfields, *Res. Dev. Note 37*, Swed. Meteorol. and Hydrol. Inst., Norrköping, 1984.

Keiding, K., F. P. Jensen, and N. Z. Heidam, Absolute modelling of urban aerosol elemental composition by factor analysis, *Anal. Chim. Acta, 181*, 79-85, 1986.

Kiehl, J. T., and B. P. Briegleb, The relative role of sulfate aerosols and greenhouse gases in climate forcing, *Science, 260*, 311-314, 1993.

Kowalczyk, G. S., C. E. Choquette, and G. E. Gordon, Chemical element balances and identification of air pollution sources in Washington, D.C., *Atmos. Environ., 12*, 1143-1153, 1978.

Lacaux, J.-P., H. Cachier, and R. Delmas, Biomass burning in Africa: an overview of its impact on atmospheric chemistry, in *Fire in the Environment: The Ecological, Atmospheric and*

Climatic Importance of Vegetation Fires, edited by P. J. Crutzen and J. G. Goldammer, pp. 159-191, John Wiley, New York, 1993.

Le Canut, P., M. O. Andreae, G. W. Harris, F. G. Wienhold, and T. Zenker, Airborne studies of emissions from savanna fires in southern Africa, 1, Aerosol emissions measured with a laser optical particle counter, *J. Geophys. Res.*, this issue.

Levine, J. S. (Ed.), *Global Biomass Burning: Atmospheric, Climatic, and Biospheric Implications*, MIT Press, Cambridge, Mass., 1991.

Lowenthal, D. H., R. C. Hanumara, K. A. Rahn, and L. A. Currie, Effects of systematic error, estimates and uncertainties in chemical mass balance apportionments: Quail Roost II revisited, *Atmos. Environ., 21*, 501-510, 1987.

Maenhaut, W., and K. Akilimali, Study of the atmospheric aerosol composition in equatorial Africa using PIXE as analytical technique, *Nucl. Instrum. Methods Phys. Res., Sect. B, 22*, 254-258, 1987.

Maenhaut, W., and J. Cafmeyer, Particle induced X-ray emission analysis and multivariate techniques: An application to the study of the sources of respirable atmospheric particles in Gent, Belgium, *J. Trace Microprobe Tech., 5*, 135-158, 1987.

Maenhaut, W., and H. Raemdonck, Accurate calibration of a Si(Li) detector for PIXE analysis, *Nucl. Instrum. Methods Phys. Res., Sect. B, 1*, 123-136, 1984.

Maenhaut, W., and J. Vandenhaute, Accurate analytic fitting of PIXE spectra, *Bull. Soc. Chim. Belg., 95*, 407-418, 1986.

Maenhaut, W., and W. H. Zoller, Determination of the chemical composition of the south pole aerosol by instrumental neutron activation, *J. Radioanal. Chem., 37*, 637-650, 1977.

Maenhaut, W., W. H. Zoller, R. A. Duce, and G. L. Hoffman, Concentration and size distribution of particulate trace elements in the south polar atmosphere, *J. Geophys. Res., 84*, 2421-2431, 1979.

Maenhaut, W., A. Selen, P. Van Espen, R. Van Grieken, and J. W. Winchester, PIXE analysis of aerosol samples collected over the Atlantic Ocean from a sailboat, *Nucl. Instrum. Methods, 181*, 399-405, 1981.

Maenhaut, W., P. Cornille, J. M. Pacyna, and V. Vitols, Trace element composition and origin of the aerosol in the Norwegian Arctic, *Atmos. Environ., 23*, 2551-2569, 1989.

Marple, V. A., K. A. Rubow, and B. A. Olson, Inertial, gravitational, centrifugal, and thermal collection techniques, in *Aerosol Measurement. Principles, Techniques and Applications*, edited by K. Willeke and P. A. Baron, pp. 206-232, Van Nostrand Reinhold, New York, 1993.

Mason, B., *Principles of Geochemistry*, 3rd ed., John Wiley, New York, 1966.

Mitchell, R. I., and J. M. Pilcher, Improved cascade impactor for measuring aerosol particle sizes in air pollutants, commercial aerosols and cigarette smoke, *Ind. Eng. Chem., 51*, 1039-1042, 1959.

Penner, J. E., R. E. Dickinson, and C. A. O'Neill, Effects of aerosol from biomass burning on the global radiation budget, *Science, 256*, 1432-1434, 1992.

Riley, J. P., and R. Chester, *Introduction to Marine Chemistry*, San Diego, Calif., 1971.

Rogers, C. F., J. G. Hudson, B. Zielinska, R. L. Tanner, J. Hallett, and J. G. Watson, Cloud condensation nuclei from biomass burning, in *Global Biomass Burning: Atmospheric, Climatic, and Biospheric Implications*, edited by J. S. Levine, pp. 431-438, MIT Press, Cambridge, Mass., 1991.

Salma, I., W. Maenhaut, J. Cafmeyer, H. J. Annegarn, and M. O. Andreae, PIXE analysis of cascade impactor samples collected at the Kruger National Park, South Africa, *Nucl. Instrum. Methods Phys. Res., Sect. B, 85*, 849-855, 1994.

Schneider, S. H., Detecting the climatic change signals: Are there any "fingerprints"?, *Science, 263*, 341-347, 1994.

Schutyser, P., W. Maenhaut, and R. Dams, Instrumental neutron activation analysis of dry atmospheric fall-out and rainwater, *Anal. Chim. Acta, 100*, 75-85, 1978.

Thurston, G. D., and J. D. Spengler, A quantitative assessment of source contributions to inhalable particulate matter pollution in metropolitan Boston, *Atmos. Environ., 19*, 9-25, 1985.

Ward, D. E., R. A. Susott, C. B. Doughty, R. Shea, C. Haskins, M. Scholes, and E. Chidumayo, Combustion efficiency and smoke emissions from fires in selected savanna ecosystems of South Africa and Zambia (abstract), *Eos Trans. AGU, 74(43)*, Fall Meet. suppl., 128, 1993.

Watson, J. G., J. A. Cooper, and J. J. Huntzicker, The effective variance weighting for least squares calculations applied to the mass balance receptor model, *Atmos. Environ., 18*, 1347-1355, 1984.

M. O. Andreae, Biogeochemistry Department, Max Planck Institute for Chemistry, P.O. Box 3060, D-55020 Mainz, Germany. (e-mail: moa@diane.mpch-mainz.mpg.de)

H. J. Annegarn, Schonland Research Center for Nuclear Sciences, University of the Witwatersrand, Private Bag 3, WITS 2050, Johannesburg, South Africa. (e-mail: annegarn@global.co.za)

J. Cafmeyer and W. Maenhaut (corresponding author), Institute for Nuclear Sciences, University of Gent, Proeftuinstraat 86, B-9000 Gent, Belgium. (e-mail: maenhaut@inwchem.rug.ac.be)

I. Salma, Research Institute for Atomic Energy, P.O. Box 49, H-1525 Budapest, Hungary. (e-mail: salma@sunserv.kfki.hu)

(Received October 31, 1994; revised August 7, 1995; accepted August 16, 1995.)